

Effects of Hyperpolarization-activated Cation Channels on Gonadotropin-releasing Hormone
Secretion

A Thesis

Presented to

The College of Graduate Studies

Austin Peay State University

In Partial Fulfillment

Of the Requirements for the Degree

Masters of Biology

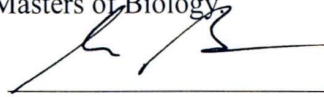
Kelsey Cleland

November, 2017

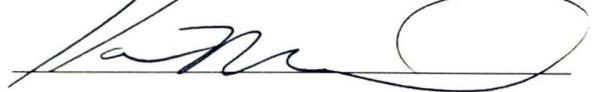
August, 2017

To the College of Graduate Studies:

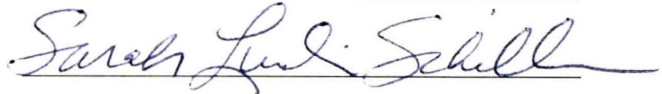
We are submitting a Thesis written by Kelsey Cleland entitled "Effects of Hyperpolarization-activated Cation Channels on Gonadotropin-releasing Hormone Secretion." We have examined the final copy of this Thesis for form and content. We recommend that it be accepted in partial fulfillment of the requirements for the degree of Masters of Biology.



Research/Committee Advisor/Chair



Committee Member



Committee Member

Accepted for the Graduate and Research Council



Dean, College of Graduate Studies

Statement of Permission to Use

In presenting this Thesis in partial fulfillment of the requirements for the Masters of Biology at Austin Peay State University, I agree that the library shall make it available to borrowers under the rules of the library. Brief quotations from this field study are allowable without special permission, provided that accurate acknowledgment of the source is made.

Permissions for extensive quotation or reproduction of this field study may be granted by my major professor, or in his/her absence, by the Head of the Interlibrary Services when, in the opinion of either, the proposed use of the material is for scholarly purposes. Any copying or use of the material in this Thesis for financial gain shall not be allowed without my written permission.

Signature



Date

12/01/2017

Effects of Hyperpolarization-activated Cation Channels on Gonadotropin-releasing Hormone Secretion

ABSTRACT

The hypothalamus contains neurons that secrete gonadotropin-releasing hormone (GnRH) into the hypophyseal portal system. This system transports GnRH to the anterior pituitary where it triggers the release of luteinizing hormone (LH) and follicle-stimulating hormone (FSH), two important gonadotropins. These hormones are key to ovulation, steroid production, and gametogenesis. GnRH is secreted in a pulsatile, or rhythmic manner, at 30 - 50 minute intervals, *in vitro*. While the mechanism of the intrinsic pacemakers remains unknown, its significance is made evident by the observation that sustained, continuous GnRH release reduces both LH and FSH secretion. Also, the frequency of GnRH release determines the relative proportions of LH and FSH secreted by the anterior pituitary. Alteration to either the amplitude or frequency of GnRH secretion affects the ability to reproduce or to maintain balance of gonadotropins. Two studies show that hyperpolarization-activated cation channels (HCN) alter the electrical activity of GnRH neurons. The hypothesis that HCN channels play a role in the control of GnRH secretion was tested by examining GnRH secretion from immortalized GnRH cells (GT1-7) before and during the blockade of HCN channels by ZD7288. ZD7288 reduced GnRH pulse frequency from 3.32 pulses/hr to 2.2 pulses/hr and from 3.2 pulses/hr to 0.833 pulses/hr in the control versus experimental and the sequential control versus experimental, respectively ($n=12$; $n=15$. $p<0.05$). The average interpeak interval (IPI) changed from 18.2 minutes to 23.1 minutes and from 17.5 minutes to 19.6 minutes in the control versus experimental and the sequential control versus

experimental, respectively ($n=12$, $p<0.05$). The total number of pulse peaks examined decreased after exposure to ZD7288 from an average of 8.9 peaks in the control to 6.6 peaks within the experimental, this was also reflected within the sequential control and experimental groups, where the average pulse peaks dropped from 6.3 to 1.7 ($p<0.05$). The results of this experiment demonstrate that HCN channels alter GnRH secretion.

TABLE OF CONTENTS

Acknowledgments.....7

Chapter

 I. Introduction.....8

 II. Literature Review.....9

 III. Methods.....24

 IV. Results.....30

 V. Discussion.....41

 VI. References.....45

Appendixes

 A. Pulse Analysis for Control Cells.....52

 B. Pulse Analysis for Experimental Cells.....65

 C. Pulse Analysis for Sequential
 Cells.....81

 D. Data Summary.....94

Acknowledgements

My heartfelt gratitude goes to my advisor, Dr. Gilbert Pitts, for his patience, motivation, and immense knowledge and the continuous support of my Master's study and related research. His guidance helped me focus during the research and writing of this thesis. I could not have imagined having a better advisor and mentor throughout my Bachelors' and Masters' courses of study.

I wish to extend my sincerest appreciations to Dr. Joe Schiller. It was with his guidance as a Graduate Assistantship Supervisor that sparked a love for teaching. He was an incredible mentor. His sense of humor and encouragement provided a continuous foundation for my initial advance into teaching.

I would like to thank Ms. Leida Perez, it was through her leadership that I was able to learn the intricacies of laboratory management, setting me on the path to success.

In addition to my advisors, I would like to thank the rest of my thesis committee: Dr. Karen Meisch, and Dr. Sarah Lundin-Schiller, for their insightful comments and encouragement, but also for the inspiration they fostered.

I must also give a special thank you to my parents and sister for their relentless encouragement, which allowed me to remain persistent when the writing process or life, in general, became difficult and demanding.

Finally, to my Fiancé, thank you for the emotional and spiritual support throughout the most difficult times of my academic career. I have the utmost respect and gratitude for my entire support network. Without you, I would not be here today.

CHAPTER I: Introduction

Gonadotropin-releasing hormone (GnRH) neurons are located in the hypothalamus and are responsible for the synthesis and pulsatile secretion of GnRH. They control fertility in vertebrates by regulating synthesis and discharge of the pituitary hormones, luteinizing hormone (LH) and follicle-stimulating hormone (FSH), which, in turn, drive gonadal steroidogenesis and gametogenesis. Thus, the secretion of GnRH fulfills a crucial role in reproduction. The objective of this study was to examine the impact of hyperpolarization-activated cation channels on the episodic secretion of GnRH.

The mechanisms that comprise the GnRH pacemaker have yet to be established. The episodic release of GnRH may be associated with the electrical bursting activity, or hyperpolarization events (Arroyo *et al.*, 2006). The diffuse and sparse nature of GnRH neurons throughout the hypothalamus, make *in vivo* studies problematic (Mellon *et al.*, 1990; Okubo, 2006; Wen *et al.*, 2008). Therefore, GT1-7 cells, a line of immortalized cells derived from transgenic mice carrying a GnRH promoter-driven oncogene (Mellon *et al.*, 1990), were used in this study to examine the role of hyperpolarization-activated cation channels in episodic GnRH secretion.

The purpose of this study was to determine the effects of hyperpolarization-activated cation channels (HCN) on the control of GnRH secretion from GT1-7 cells. This will provide further insight into the connections between cellular electrical activities and their role in effecting major cellular functions, such as hormonal secretions. This is important and necessary in understanding the integral components which effect the neuroendocrine axes, and thus, control main physiological functions such as growth, development, and reproduction.

CHAPTER II: Literature Review

Introduction

GnRH neurons directly impact reproduction and fertility in diverse type of animals (Arrow *et al.*, 2006, Biel *et al.*, 1999; McCormick, & Pape, 1990, Marshall *et al.*, 1992). The frequency of GnRH pulses is the key to successful regulation of reproduction. However, the mechanisms which drive the GnRH pacemaker are poorly understood.

This literature review will first frame the overarching impact of GnRH by describing the hypothalamic-pituitary-gonadal axis (HPG axis), and the role of GnRH. This topic will be followed by a description of the GnRH regulation in neurons and GT1-7 cells. Then, the mechanisms comprising the pacemaker will be described as well as the case for the role of hyperpolarization-activated cation channels.

Hypothalamic-Pituitary-Gonadal Axis

Mammalian reproduction is controlled by integrated interactions between the hypothalamus, pituitary, and gonads. Each component is regulated by feedback mechanisms to coordinate steroidogenesis and gametogenesis (Lacau-Mengido *et al.*, 1998).

GnRH plays a critical role in the HPG axis, in fact, it is often described as being the final common pathway for the control of reproduction (Marshall *et al.*, 1992; Jayes *et al.*, 1997; Sliwowska *et al.*, 2014). GnRH soma are located in the preoptic area and basal hypothalamus

and episodically release GnRH into the hypophyseal portal blood at the median eminence (Moenter *et al.*, 1992). The portal blood carries GnRH to the anterior pituitary gland where it induces the release of follicle-stimulating hormone (FSH) and luteinizing hormone (LH). The frequency of GnRH secretion is responsible for the differential secretion of LH and FSH (Schally *et al.*, 1971). These hormones, in turn, regulate the production of gonadal steroids, such as estradiol and testosterone, and are also involved in gamete maturation (Lacau-Mengido *et al.*, 1998; Schally *et al.*, 1971). Thus, GnRH is responsible for the adequate production of sex hormones and the proper functioning of the reproductive system.

While GnRH regulates FSH and LH in both males and females, the frequency of GnRH pulses remains continuous in males following puberty (Lacau-Medgido *et al.*, 1998). However, the frequency of GnRH pulses fluctuates throughout the female reproductive cycle (Schauer *et al.*, 2015). At the start of both the estrous and menstrual cycle, GnRH pulse frequency and amplitude are both low (Schally *et al.*, 1971; Lacau-Medgido *et al.*, 1998). Low frequency GnRH pulses increase FSH secretion from the anterior pituitary which then stimulates ovarian follicle recruitment and maturation (Schally *et al.*, 1971; Lacau-Medgido *e. al.*, 1998). As ovarian follicles develop, they secrete more estradiol (Schally *et al.*, 1971; Lacau-Medgido *et al.*, 1998). As ovulation approaches, GnRH pulse frequency and amplitude increase (Schally *et al.*, 1971; Lacau-Medgido *et al.*, 1998). When estradiol levels reach a certain threshold it starts to exert positive feedback on GnRH (Lacau-Medgido *et al.*, 1998). The increase in GnRH frequency, coupled with the positive feedback effects of estrogen lead to a surge in LH that initiates ovulation. At this time the luteal phase begins, and the corpus luteum produces progesterone, which provides a negative feedback, reducing the production of GnRH (Schally *et al.*, 1971).

Several studies have shown the relationship between GnRH pulse frequency and the ratio of LH to FSH secretion. High frequency GnRH pulses (1/hr) result in high plasma LH baselines and low pulse amplitudes, while low frequency GnRH pulses (0.25/ hr) result in low LH baselines and high LH pulse amplitudes (Jayes *et al.*, 1997; Jacob *et al.*, 2001; Clarke and Cummins, 1985). Jayes *et al.*, (1997), used gilts to show that the pituitary gland was sensitive to changes in GnRH pulse stimulation. Where low GnRH pulse frequency induced FSH secretion, high pulse frequency induced LH secretion; estrogen (E) can influence LH pulse frequency by altering the release of the gonadotrophs by GnRH (Jayes *et al.*, 1997; Clarke and Cummins, 1985).

FSH, LH, and E are components of feedback loops that regulate reproduction. The release of GnRH is inhibited by estrogen (E) negative feedback before the onset of puberty and during most of the female reproductive cycle. On the other hand, the release of GnRH, which is a major requirement for ovulation, is stimulated by E- mediated positive feedback (Schally *et al.*, 1971, Ordog *et al.*, 1995).

As ovarian follicles are recruited for maturation, estradiol levels slowly rise. During proestrus, a positive feedback mechanism on GnRH is applied as estradiol levels increase (Lacau-Medgido *et al.*, 1998). This prompts an increase in the frequency and amplitude of GnRH pulses, which prompts the LH surge and ovulation. After which, the luteal stage is started, and the corpus luteum creates progesterone, which instigates a negative feedback mechanism on GnRH generation (Schally *et al.*, 1971).

In the ovine luteal phase, GnRH is emitted as low-frequency pulses, which change to high-frequency, low-amplitude pulses in the mid-follicular stage. Later, E-mediated positive

feedback induces a high-amplitude GnRH secretion which causes the LH surge during the late-follicular stage (proestrus)(Chappell *et al.*, 2000). Curiously, in the sheep but not in the macaque or rodent, the GnRH surge proceeds long after the LH surge has ended, showing that the gonadotrophs desensitize to the GnRH surge contribution in sheep, ending the LH discharge before negative feedback restraint of GnRH emission. In ovariectomized ewes, the GnRH and LH pulse amplitudes increase and episodic frequency diminishes (Chappell *et al.*, 2000). 17β -estradiol (E2) treatment fundamentally decreases the GnRH and LH pulse amplitude, yet increases episodic pulse frequency, prompting a general diminishment in GnRH and LH secretion before the GnRH and LH surge (Chappell *et al.*, 2000; Clarke *et al.*, 1984). These discoveries would show there are essential changes in GnRH pulse frequency and amplitude amid the distinctive phases of the ovulatory cycle (Clarke *et al.*, 1984). In ovariectomized ewes and rhesus monkeys with arcuate nucleus lesions treated with episodic exogenous GnRH to alter the pulse frequency and amplitudes of GnRH, both frequency and amplitude of LH correlates with changes in GnRH (Clarke *et al.*, 1984).

Pulsatile LH has been utilized as a surrogate marker of GnRH pulses. LH emission is pulsatile, while FSH is not (Hall *et al.*, 2000). LH levels can be effectively measured in jugular blood and used to estimate GnRH levels (Hall *et al.*, 2000). The relationship between GnRH and LH pulses can be used to examine the input of gonadal hormones in various physiological circumstances (Vidal *et al.*, 2012). Vidal *et al.*, (2012), worked to develop an algorithm (dynpeak) to detect experimental hormonal pulse peaks and interpeak intervals (IPI) of the neuroendocrine axis. The dynpeak software was tested using synthetic and experimental LH secretions, in order to standardize and test the accuracy of the algorithm. The experimental tests were performed on two experimental groups, 10 estrous-synchronized ewes and 9

ovariectomized ewes. Jugular blood was collected every 10 minutes for 24-hr periods. Blood plasma was then assayed for LH levels (ng/mL/min.). This allowed for the introduction of uncertainty on both the measured LH level, to assess the effects of assay variability, and the time of measurement, to account for hidden variability in sampling chronology, to ensure the ability of event detection was not an effect of noise (Vidal *et al.*, 2012). The validity of the pulse detection has already been validated in investigations of the midcycle surge in women (Hall *et al.*, 2000). In this study, researchers tested the effect of age on GnRH secretions, using two groups of healthy post-menopausal women (45-50; 70-80yrs) (Hall *et al.*, 2000). To establish changes in GnRH pulse frequency, two hormonal markers for GnRH were used, LH and gonadotropin free α -subunit (FAS). Blood plasma was collected at varying time intervals to test the efficacy of surrogate markers, at 5, 10, and 15 minute intervals for 12hr periods (Hall *et al.*, 2000). Although, testing recurrence of each LH at 5 minute intervals was required for significant identification of GnRH pulse frequencies (Hall *et al.*, 2000).

The GnRH Pacemaker

GnRH neurons have an intrinsic pacemaker that produces GnRH pulses at a frequency of 0.5 pulses/h to 1 pulse/h (Moenter *et al.*, 1992; Nunemaker *et al.*, 2003). Schauer *et al.*, 2015 showed that GnRHR (neurons with active GnRH receptors) neurons synchronized their action potential producing activity with the female estrous cycle (Figure 1). With the use of *in-vivo* treatment with a well-established GnRHR antagonist, cetrorelix, Schauer *et al.*, 2015 showed cetrorelix is capable of affecting the activity of GnRHR neurons in the brain. GnRH induces burst firing in hypothalamic GnRHR neurons, modulating the female reproductive cycle (Figure

1) (Schauer *et al.*, 2015). Through GnRH stimulation, the activity of GnRHR neurons change from tonic to burst firing, an effect that is reversed by cetorelix (Figure 1) (Schauer *et al.*, 2015).

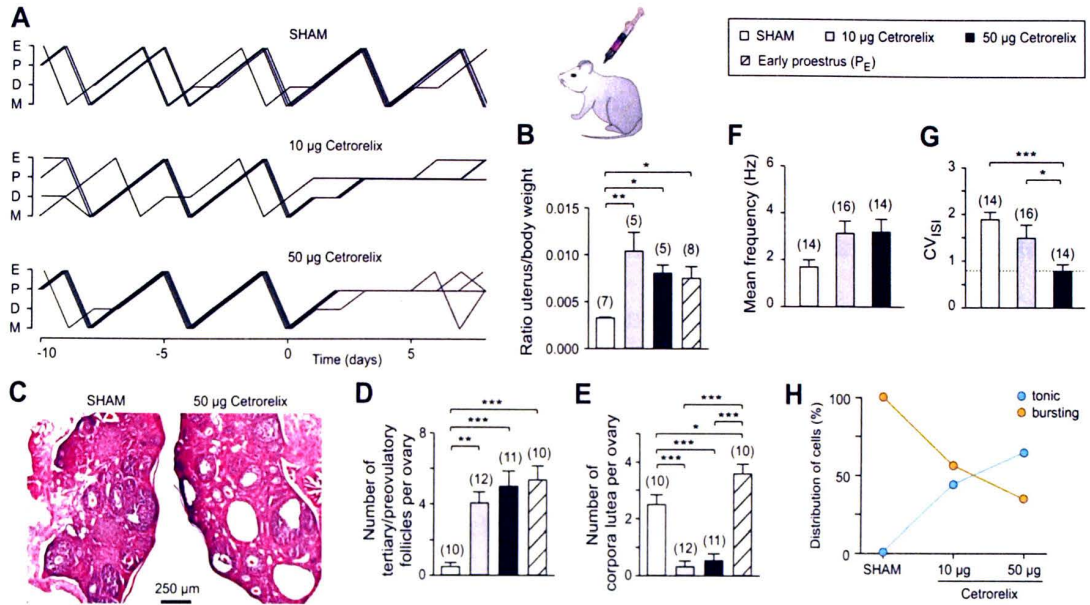


Figure 1: *In-Vivo* subcutaneous injections of GnRHR antagonist, 10-50 µg cetorelix modulates female mouse reproductive cycle (A/B). Sham vs cetorelix effects the development of tertiary follicles and corpora lutea within female mice (C/D/E). Cetorelix effects neuronal firing of GnRHR neurons throughout the female reproductive cycle of mice (F/G) (Schauer *et al.*, 2015).

This implies that electrical activity may drive GnRH release. The resting membrane potential and the triggering of the action potential are regulated through a complex system of ion channels in GnRH neurons (De La Escalera *et al.*, 1992; Moenter *et al.*, 1992; Nunemaker *et al.*, 2003).

There are two main mechanisms by which the neuronal membrane potential can depolarize past the threshold for an action potential, synaptic conductance and intrinsic changes in ion conductance (Moenter *et al.*, 1992; Nunemaker *et al.*, 2003). Since isolated cultures of

GnRH neurons continue to produce spontaneous bursts of action potentials, this suggests that synaptic conductance is not necessary for GnRH neuron action potential production (Kuehl-Kovarik *et al.*, 2002). Interestingly, mammalian GnRH neurons also exhibit a high input resistance (R_{in}), around one gigaohm (Kuehl-Kovarik *et al.*, 2002). Because GnRH R_{in} is high, small changes in ion or cation conductance have greater effects on the membrane potential, which can contribute to the intrinsic firing potentials (Kuehl-Kovarik *et al.*, 2002). There are several currents that could have an effect on the intrinsic ion conductance, T-type calcium currents, calcium-activated potassium currents, sodium currents, and hyperpolarization-activated cation currents (I_h). Hyperpolarization-activated cation channels are the focus of this study.

Hyperpolarization-Activated Cation Channels

Hyperpolarization-activated cation channels (HCN) are one of many types of ion channels that have been identified in GnRH neurons (Arroyo *et al.*, 2006). These channels effect membrane permeability to both Na^+ and K^+ ions, with a Na^+/K^+ permeability ratio of about 0.27 (Biel *et al.*, 2009). In other cell types, HCN channels have been associated with a determination of the resting membrane potential, integration of postsynaptic potentials, and the generation of biological rhythms (Biel *et al.*, 2009; DiFrancesco *et al.*, 1981). Therefore, it is entirely possible that these channels may play a role in generating the rhythmicity of GnRH secretion.

The standard structure among HCN channels is depicted in Figure 2. There are four HCN channel types, all of which exhibit the same properties, in varying degrees of efficacy (Emery *et al.*, 2012). HCN channels have both voltage and ligand gates. Where, when cAMP is bound to the cyclic nucleotide binding domain (CNBD), voltage sensitivity increases, allowing increase in

the Na^+ influx at the resting potential (Emery *et al.*, 2012). Blocking of the HCN channel by ZD7288 significantly suppresses episodic firing of the neuron (Emery *et al.*, 2012).

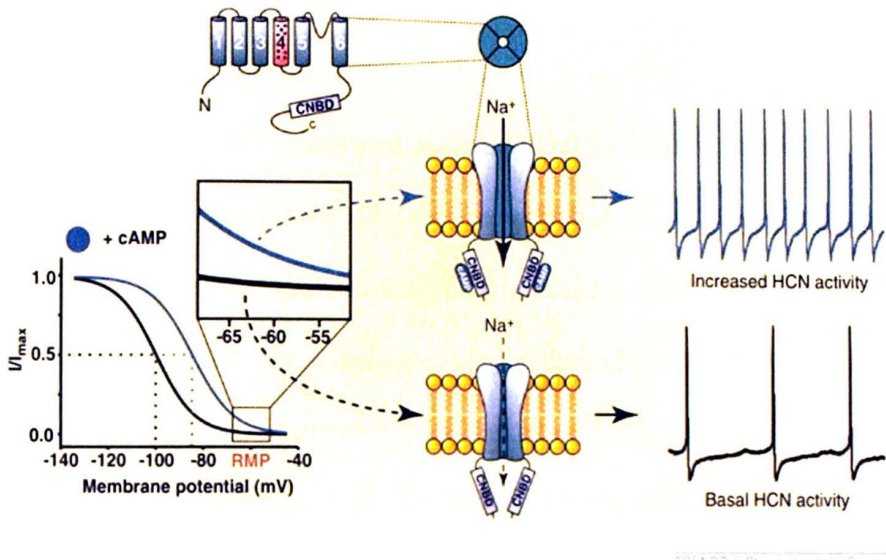


Figure 2: The structure of HCN channels (HCN2). Binding of cAMP shifts voltage dependence, increasing the inward ionic current (top left), increasing the neuronal activity (Emery *et al.*, 2012).

HCN channels are more permeable to K^+ than to Na^+ , with permeability ratios of about 4:1. Furthermore, the membrane current increases with extracellular K^+ concentration and decreases with a reduction in extracellular Na^+ concentration (Chu *et al.*, 2010; DiFrancesco *et al.*, 1981). A gradual hyperpolarization of the membrane voltage causes opening of the HCN channel around -75mV to -130mV (Chu *et al.*, 2010). Opening of hyperpolarization-activated cation channels leads to an inward Ca^{2+} current and outward K^+ current, termed I_h (Chu *et al.*, 2010; Yu *et al.*, 2004). Although HCN channels display a very low permeability to Ca^{2+} , compared to other Ca^{2+} permeable channels, it is this inward current that helps reset the resting membrane potential, creating the possibility of oscillating hyperpolarization events (Yu *et al.*,

2004) by increasing the rate of repolarization of the cell membrane, after an action potential, resetting the neuron for another action potential to occur (Chu *et al.*, 2010).

All HCN channel types (HCN1-4) exhibit the basic biophysical properties of the pacemaker current (Yu *et al.*, 2004). These channels contribute to the control of rhythmic firing in cardiac and neuronal cells, regulation of neuronal excitability by modulating the cell membrane resting potential and decreasing the after-hyperpolarization event (AHP), and sensory transduction through oscillating Ca^{2+} influxes, leading to an increase in action potentials (Yu *et al.*, 2004; Chu *et al.*, 2010). The different channel types vary in their characteristics. For example, all HCN channels are activated through hyperpolarization of the cell membrane, but some have varying degrees of sensitivity and dependence to cAMP and voltage-activation, where HCN1 and HCN3 are weakly effected by cAMP, while HCN2 and HCN4 have activation thresholds that are +15mV higher through cAMP (Yu *et al.*, 2004; Chu *et al.*, 2010).

HCNs are responsible for rhythmic activities in various tissues, such as cardiac cells and neurons (Yu *et al.*, 2004). Several HCN channels have been reported in GnRH neurons located within the hypothalamus of female rats and mice as well as GT1-7 cells (Biel *et al.*, 1999; Arroyo *et al.*, 2006). HCN2 and HCN3 are expressed in endogenous GnRH neurons in the rat hypothalamus, although HCN1-4 channels were not present in GnRH nerve fibers in the median eminence of the rat hypothalamus. Arroyo *et al.* (2006), suggested that HCN2 and HCN3 channels could be responsible for the pacemaker mechanism, since these channels are present in GnRH neurons; with HCN3 being expressed in greater quantity compared to HCN2.

HCN channels possess inherent negative-feedback mechanisms to disrupt hyperpolarization and deactivate channels. This is due to the ability of inward currents to re-

establish resting membrane potential; thereby, deactivating the HCN channel. Through either the increase or the decrease of cAMP, neurotransmitters can directly modulate the activation kinetics and maximal current of HCN channels. Differing HCN channels are affected in varying degrees by cAMP, for example HCN2 activation shifts 2-7 mV and HCN3 with no shift observed (Biel *et al.*, 2009). This suggests there are other factors modulating the GnRH pacemaker through the activation of HCN channels.

Modulation of the GnRH Pacemaker

Neural and endocrine inputs such as kisspeptin (KISSPEPTIN) and estrogen can alter the secretory pattern of GnRH. Estrogen has been observed to inhibit GnRH and LH secretion, in ovariectomized (OVX) mice (Zhang *et al.*, 2013). However, 12-48hrs later, estrogen elicited positive-feedback effects to increase GnRH, leading to the LH surge (Zhang *et al.*, 2013). The mechanisms by which these effects are elicited help to mediate the HPG axis and regulate GnRH secretion (Han *et al.*, 2005). KISSPEPTIN is one of the most excitatory neurotransmitters of GnRH neurons and is regulated by estrogen (Zhang *et al.*, 2013; Chappell *et al.*, 2000).

Estrogen has a role in the positive feedback mechanism altering GnRH secretion. Estrogen (E) stimulates GnRH surges through the activation of the progesterone receptors (PR) in the anteroventral periventricular (AVPV) region of the hypothalamus (Chappell *et al.*, 2000). In these experiments, ovariectomized (OVX) E2-primed rats were treated with estradiol benzoate or oil vehicle. Only the estradiol treated rats produced synchronous GnRH and LH surges (Chappell *et al.*, 2000). This shows that PR activation in the AVPV is necessary for the stimulation of GnRH surges by E2 (Chappell *et al.*, 2000).

Castration experiments on mice proved that there was an increase in GnRH discharge along with the increase of I_h in GnRH neurons when compared to intact-gonadal male mice (Chu *et al.*, 2010). Testosterone in male gonads can be converted to estradiol, allowing the occurrence of negative feedback signals to decrease GnRH secretion in the hypothalamus and GnRH neuron activity. Estradiol decreased I_h levels when introduced into castrated male mice, restoring I_h amplitudes to those comparable with intact-gonadal male mice (Chu *et al.*, 2010). This finding confirms the idea that I_h is involved in the negative feedback mechanism. Whether estradiol directly or indirectly effected GnRH neurons remains unknown (Chu *et al.*, 2010). It has been found that homeostatic control depends upon the frequency of GnRH release (Keenan *et al.*, 2011).

Estrogen may elicit more direct effect on GnRH neurons, while simultaneously effecting KISSPEPTIN. Estrogen stimulates Kiss1 mRNA expression in this brain region (Han *et al.*, 2005). Kisspeptin neurons, located in the anteroventral and more caudal periventricular preoptic area (AVPV/PeN), are in direct contact with GnRH cells, and express the estrogen receptor alpha ($ER\alpha$). At least 50% of GnRH neurons receive monosynaptic input from the AVPV/PeN neurons, suggesting Kiss1 neurons may be presynaptic pacemaker neurons modulating GnRH neurons through synaptic conductance (Zhang *et al.*, 2013). Stimulation of these AVPV/PeN neurons delayed excitatory response in GnRH neurons, which was observed to be blocked through kisspeptin-inhibitory peptides (Zhang *et al.*, 2013). Furthermore, Kiss1 neurons are sensitive to estrogen since estrogen produces an I_h current in Kiss1 cells, releasing KISSPEPTIN, subsequently providing an excitatory drive for GnRH hyperpolarization and the estrogen-stimulated LH surge (Han *et al.*, 2005; Zhang *et al.*, 2013).

Animal studies have provided evidence that KISSPEPTIN works upstream in the AVPV and Arc nuclei to enhance GnRH secretion (Smith *et al.*, 2008). Kisspeptin (Kiss1) neurons produce action potentials capable of activating HCN channels and T-type calcium channels (Zhang *et al.*, 2013). Under voltage clamp conditions, these channels increase potassium permeability causing hyperpolarization under current clamp conditions (Kelly *et al.*, 2013). Exogenous KISSPEPTIN has also been shown to stimulate GnRH secretion from hypothalamic explants and has been shown to increase the production of both GnRH and LH in ewes when applied by introcerebroventricular infusion (Messenger *et al.*, 2005; Thompson *et al.*, 2004). Furthermore, the role of KISSPEPTIN as a modulator of GnRH was supported by KISSPEPTIN-antagonistic studies, when KISSPEPTIN-antagonist was injected into the median eminence of rhesus monkeys, both the GnRH pulses and tonic GnRH secretions were suppressed (Roseweir *et al.*, 2009). This suggests that KISSPEPTIN works to modulate GnRH pulsation to effect LH secretions downstream of the HPG axis.

ZD7288 stops Hyperpolarization

Researchers have searched for HCN antagonists since 1979 when Brown (1979) found that adrenaline quickens heart rate via its actions on hyperpolarization-activated cation channels. More than ten years later, ZD7288 [4-(N-Ethyl-N-phenylamino)- 1,2 dimethyl-6-(methylamino) pyrimidinium chloride ICI-D7288 N-Ethyl-1,6-dihydro-1,2-dimethyl-6-(methylimino)- N-phenyl-4-pyrimidinamine hydrochloride] was reported to be a profoundly specific blocker of HCN as it reduced heart rate without impeding cardiovascular capacity (Luo *et al.*, 2007). Since then, ZD7288 has been broadly utilized as a specific HCN inhibitor (Wu *et al.*, 2012).

In the previous three decades, additional drugs with heart rate diminishing properties have been produced and recognized as HCN channel blockers. Early medications recognized as immaculate bradycardic operators include alinidine (ST567), ZD7288 and zatebradine (UL-FS49) and its subordinates; ivabradine (S16257) (Wu *et al.*, 2012). The principle activity of these substances is to diminish the diastolic depolarization incline by blocking HCN channel current. Ivabradin can only target HCN channels intracellularly, or when the channel opens intracellularly (Luo *et al.*, 2007; Wu *et al.*, 2012). Zatebradine is a structural isoform to ivabradin but only elicits effects in a voltage-dependent manner, but does not display current-dependency (Luo *et al.*, 2007). This suggests that they have different binding sights to the HCN channel.

ZD7288 elicits its effects in a current-dependence as well as voltage-dependence mechanism (Wu *et al.*, 2012). While localizing the blocking impact of ZD7288 on I_h in dorsoal root ganglion (DRG) neurons, by isolating ZD7288 administration through the use of a glass pipette during channel recordings, it was found that high concentrations (more than 100 μM) of ZD7288 reduces calcium ion influx. Subsequently, the impacts of ZD7288 reduce the cells ability to recover from after-hyperpolarization, and cellular hyperpolarization by means of the HCN channels (Wu *et al.*, 2012). ZD7288 did not alter the rate of rise and the span of action potentials in quick spiking interneurons, implying that it does not influence voltage-gated Na^+ and K^+ channels. Additionally, ZD7288 did not change the firing of action potentials activated by quick use of GABA, demonstrating that it does not influence GABA receptors (Aponte *et al.*, 2006). Therefore, ZD7288 elicits its effects through pharmacological specificity on HCN channels without effecting neighboring intermembrane protein channels (Wu *et al.*, 2012; Aponte *et al.*, 2006).

GT1-7 Cells

GT1-7 cells, an immortalized line of GnRH neurons, were used in this experiment since the perfusion of primary GnRH neuron cell cultures does not provide adequate levels of GnRH to measure. These cells are self-adherent and have biophysical properties expected of GnRH neurons, including rhythmic action potentials and episodic secretion of GnRH (Mellon *et al.*, 1990). Studies by Mellon *et al.*, 1990 and Silverman 1988 showed that GT1-7 cells spontaneously secrete GnRH in a pulsatile manner with pulses at 25.8 minute intervals, and a mean duration of 18.8 minutes. However, the amplitude of GnRH pulses is greater than that seen *in vivo* (Mellon *et al.*, 1990; Silverman *et al.*, 1988). Generally, the pattern of GnRH discharge is determined by afferent and intrinsic processes. The episodic activity of GnRH neurons is found within isolated GnRH cell cultures and persist in absence of other cell types.

The capacity of GT1-7 cells to display periodic GnRH discharge without the influence other cell types, demonstrates that a native pacemaker produced through intrinsic ion currents, could be a significant factor affecting pulsatile GnRH discharge (Funahashi *et al.*, 2003). According to Funahashi *et al.* (2003), the pulsatile secretion of GnRH from typical and immortalized GnRH neurons is profoundly dependent on calcium ion and fortified by cAMP. Ca^{2+} influx helps the after hyperpolarization (AHP) rebound for the possibility of another AP to occur; after hyperpolarization, the Ca^{2+} influx helps repolarize the cell membrane, resetting the HCN channels and creating the opportunity of oscillations of hyperpolarizing events (Funahashi *et al.*, 2003).

GT1-7 cells used in this study demonstrate GnRH discharge upon depolarization with veratridine or high quantities of potassium ions. In the study of De Escalera *et al.* (1992), the application of the cells with tetrodotoxin, which is a type of blocker for rapid sodium channels, hinders the activity of veratridine. Moreover, treatment with tetrodotoxin fundamentally restrains

60% of the GnRH discharge, proposing that GT1-7 cells are fit for creating unconstrained propagated activity potentials which lead to hormone emission (De Escalera *et al.*, 1992). Understanding the ability of GT1-7 cells to produce large unconstrained secretions of hormones can be used as a tool to determine cell viability, after experimentation with cell cultures. The large quantity of hormone production can be used as a marker to determine if cells survived exposure to drugs, such as ZD7288.

Conclusion

GnRH is a neurohormone critical in maintaining the balance and response of intricate feedback loops corresponding to the HPG axis. The HPG axis regulates sex steroid and hormonal feedback in many living organisms from tunicates to mammals (McCormick, & Pape, 1990, Marshall *et al.*, 1992). Thus, GnRH is a critical component in regulating fertility of many different organisms (McCormick, & Pape, 1990, Marshall *et al.*, 1992). However, the mechanisms modulating GnRH secretions have yet to be fully elucidated. GnRH is responsive to many factors which may coordinate hormonal release, such as estrogen and kisspeptin (Zhang *et al.*, 2013; Chappell *et al.*, 2000). A common link between these factors and GnRH neurons could be the potential for HCN channels to regulate the cell membrane voltage through the flow of ions. This could explain GnRH neuronal capabilities to produce episodic action potentials in isolated cell cultures, while supporting the regulatory effect of E and conductance from kisspeptin neurons.

CHAPTER III: Methods

Cell Culture

GT1-7 cells were received from Dr. Pamela Mellon at the University of California, Berkeley. The cells were cultured at 37°C in 5% CO₂. The cells were grown in 100 mm poly-D lysine-coated tissue culture dishes (BD Falcon, Franklin Lakes, NJ; Catalog # P35GC-1.0-14-C). GT1-7 cells were grown to 90% confluence in medium composed Dulbecco's Modified Eagle Medium, DMEM/F12 (DMEM/F12; Invitrogen, Grand Island, NY; Catalog # 12634-010) supplemented with 10% heat-inactivated fetal calf serum, inoculated with a 1% concentration of penicillin/streptomycin (100 µg/ml; 100 µg/ml; Invitrogen, Catalog # 1037 8016, respectively). One million GT1-7 cells were placed into each of six wells of a 12-well plate (Thermo Scientific, Catalog # 150200) and grown to 90% confluence before being serum-starved with Opti-Mem medium (Invitrogen, Catalog # 11058021) for 24 hours (Figure 3).

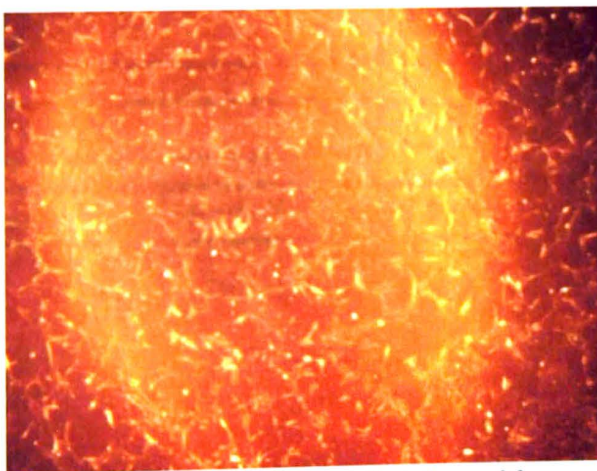


Figure 3. Image of GT1-7 cells taken with a compound microscope. The cells are approximately 60% confluent. The culture was magnified 400X.

Experimental Design

The control group consisted of 6 wells that were simultaneously perfused with only Locke's medium at a rate of 100 μ l/minute using a Brandel Suprafusion 1000 perfusion system (Brandel, Inc., Gaithersburg, MD); the experimental group consisted of 6 wells simultaneously perfused with 50 μ M ZD7288 (Tocris, Catalog # 1000) dissolved in Locke's medium. Each treatment continued for 180 minutes. Perfusate samples were collected at four-minute intervals from both the control and experimental groups. After 180 minutes, all cells were perfused with 0.1 mM veratridine (Sigma, St. Louis, MO, Catalog # V5754) for 20 minutes to determine cell viability. A sequential control group received only Locke's medium for 120 minutes at which time a sequential experimental group received 50 μ M ZD7288, administered for an additional 120 minutes. Again, the cells were treated with 0.1 mM veratridine for 20 minutes. The experimental design is depicted in Figure 4. Perfusate samples were stored at -20°C until they could be assayed for GnRH.

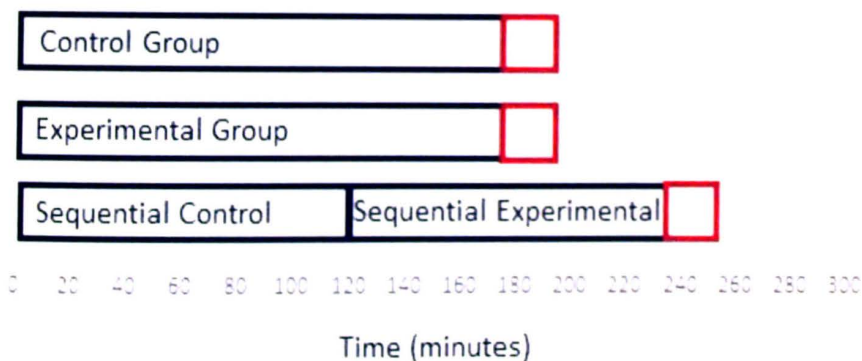


Figure 4. Experimental Design. The control group received Lockes medium for 180 minutes and the experimental group received ZD7288 for 180 minutes. Another group received Lockes medium (sequential control) for 120 minutes followed by ZD7288 (sequential experimental) for another 120 minutes. At the end of each experiment, each group was perfused with veratridine for 20 minutes (red boxes).

Control runs were repeated until samples were collected from a total of 12 individual tissue culture wells. Experimental runs were repeated to obtain 15 individual wells. Sequential groups were repeated twice, for a total of 12 separate wells.

GnRH Enzyme Immunoassay

Enzyme immunoassays were performed to measure GnRH. The assay was a modified version (Farsian *et al.*, 2008) of an assay developed by Tsai *et al.*, 2003. Ninety-six well plates were pre-coated with 100 μ l of 5 μ g/ml donkey anti-rabbit antibody (Jackson Immuno Research, West Grove, PA) in 0.1 M coating buffer (0.1 M NaHCO₃; 0.1 M Na₂CO₃; pH 9.5) and left to incubate overnight at room temperature. The wells were rinsed twice with assay buffer (0.1 M sodium phosphate buffer, pH 7.8; 0.15 M NaCl; 0.1% Tween 20), then washed three times in assay buffer, letting the wash incubate for one minute between each wash. Each well was completely emptied by aspirating any remaining solution, twice, then coated with 100 μ l of anti-GnRH primary antibody (R1245 from University of Colorado Boulder, diluted 1:50 in assay buffer), then left to incubate, shaking, overnight at 4 °C. Following incubation, wells were rinsed twice and washed three times, as described earlier, then any remaining solution was removed. Standards and unknown samples (100 μ l) were added to the wells in triplicate, and incubated overnight, shaking, at 4 °C. Following incubation, the plates were left shaking until warmed to room temperature. Biotinylated GnRH (50 μ l, Bachem, Catalog # H-4792; diluted 4:10000 in assay buffer) was added to the wells and allowed to incubate for an hour, shaking, at room temperature. The wells were washed three times (shaking between each wash for one minute)

with assay buffer and emptied completely. Avidin D-horseradish peroxidase (Vector Laboratories, Catalog # A-2004; 100 μ l, diluted 2:10000 in assay buffer) was added to each well and left to shake for one hour at room temperature. The wells were washed eight times (shaking for one minute between each wash), before 100 μ l of Supersignal Substrate (Pierce, Catalog # 37075) was added to each well and left to incubate for 4 minutes, shaking, at room temperature.

All samples were analyzed for chemiluminescence using Bio-Tek Synergy HT plate reader at 562 nm. For each assay, a standard curve was created, using an intra-assay CV, based on the known concentrations of a standard dilution and GnRH free buffer (starting at 100 pg, diluted to zero at 33.33 pg steps). This provided the minimum detectable GnRH concentration for analysis. Sample doses were calculated using the four-logistics parameter curve fit.

Data Analysis

Dynpeak pulse analysis software was used to determine GnRH pulse parameters, by entering each recorded value above the minimum detectable GnRH concentration for an entire run into the software program (Provided by Pauline Campos; <http://www.scilab.org/fr>) (Vidal *et al.*, 2012). This work was originally coded for the analysis of LH hormone parameters, but with edits to LH peaks, can be used to express a "true" GnRH pulse peak (Figure 2). The “pind=lhpeaks(sig, T);” edited to “pind = gnrhpeaks(sig, T);” composes the algorithm used to measure the average amplitude and duration of pulse peaks, to determine which are inter-peak pulses and which are true pulse peaks (Figure 3). The code was changed so the titles of the peaks were identified as GnRH instead of LH by substituting “interactive_gnrhpeaks” for “interactive_lhpeaks” (Figure 5). The true interpeak interval (IPI) values were calculated with

Dynpeak. The software also utilized a moving cubic function to fit the values of the IPI series into a tunnel of expected peaks throughout each series. Unusually high pulse peaks, outside of the tunnel, could suggest that there were multiple ‘true’ GnRH secretory events that occurred in a short time frame, and results in one large pulse peak being detected. Pulse peaks occurring below the tunnel, signify a low probability of a true secretory event. GnRH pulses that fell outside GnRH tunnel were not counted as pulse. Peaks after veratridine exposure were not included, but noted for cell viability.

```
// Detect peaks
sig = [ X; X; X; . . . ]
T=3;
pind = gnrhpeaks(sig, T);
t=(1:size(sig,'*'))*T;
clf;
plot(t,sig,'-b',t(pind),sig(pind),'or');
interactive_gnrhpeaks
```

Figure 5. GnRH-specific coding for Dynpeak pulse analysis program.

Each peak was graphed and marked with a vertical line passing through the center of the peak. The number of peaks was counted by the investigator and recorded for comparison of the treatments. Any peaks existing outside of the GnRH tunnel, in panel B composed by the Dynpeak software were not included in the total number of GnRH peaks, as they represent possible outliers of true pulse peaks.

Statistical analysis was performed using JMP statistical analysis software, provided by APSU. Interpeak intervals and changes in the amplitude of GnRH secretion of treated and

untreated groups were compared using two-sample t-tests at a significance of $p < 0.01$. Interpeak intervals and the over-all number of peaks present within the sequential groups were also compared using a two-sample t-test at a significance of $p < 0.01$.

CHAPTER IV: Results

The HCN-specific blocker ZD7288 was used in this experiment to determine if HCN channels play a role in the episodic secretion of GnRH. Three groups were compared to determine the effects of ZD7288 on GnRH secretions; the control group received only Locke's medium for 180 minutes; the experimental group received ZD7288 dissolved in Locke's medium for 180 minutes; and the sequential groups, receiving Locke's medium for the first 120 minutes and ZD7288 for an additional 120 minutes. Each group received 0.1 mM veratridine at the end of each run to determine cell viability. Cultures that did not respond to veratridine were left out of the experimental analysis.

The figures in Appendix A-C depict the amounts of GnRH secreted by individual cultures (wells) during the course of the study. Control wells are pictured in Appendix A. Cultures receiving ZD7288 are depicted in Appendix B and the sequential groups are depicted in Appendix C.

Comparison of the control and experimental groups, during which Locke's medium or ZD7288 were continuously perfused over GT1-7 cells revealed that the ZD7288 significantly impacted the number of GnRH pulses (Figure 6, control: 18.9 ± 0.357 pulses; experimental: 6.6 ± 0.335 pulses, $p < 0.05$). In addition, the average interpeak interval significantly differed between the groups (Figure 7, control: 18.2 ± 0.911 minutes; experimental: 23.1 ± 0.813 minutes; $p < 0.05$).

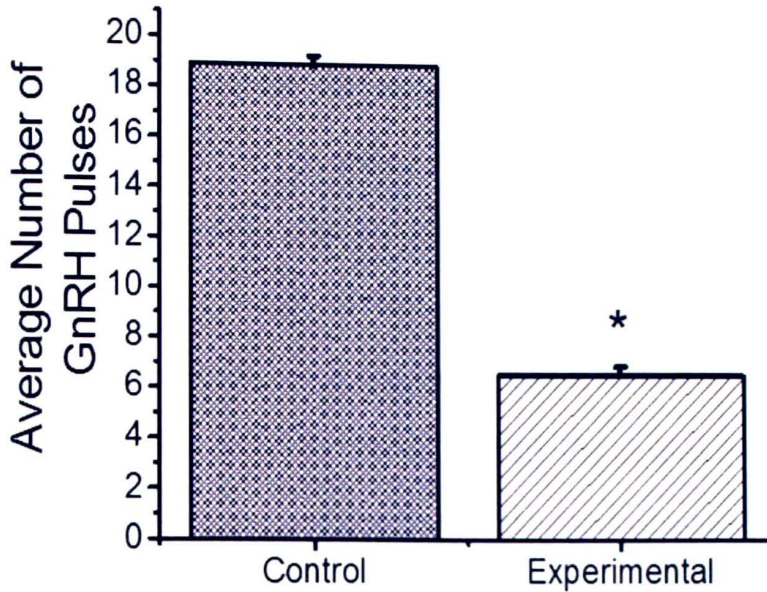


Figure 6: Average number of GnRH peaks from the control and experimental perfusions. ZD7288 significantly altered the number of GnRH peaks during the 120 minute experiment (Control: 18.9 ± 0.357 pulses, $n=12$; Experimental: 6.6 ± 0.335 pulses, $n=15$, $p < 0.05$).

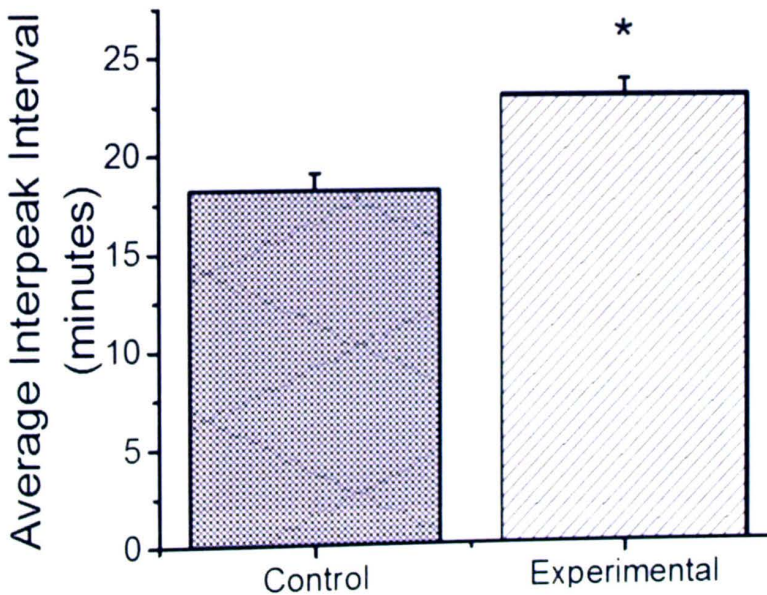


Figure 7: The average interpeak intervals during the control and experimental perfusions. ZD7288 significantly altered the duration between GnRH peaks during the 120 minute experiment (Control: 18.2 ± 0.911 minutes, $n=12$; Experimental: 23.1 ± 0.813 minutes, $n=15$, $p < 0.05$).

In addition to examining the effects of continuous medium perfusion, we tested what would happen upon switching from Locke's medium to ZD7288. Comparison of the sequential cultures, during which Locke's medium was perfused over GT1-7 cells for 120 minutes, then ZD7288 was added for an additional 120 minutes revealed that the ZD7288 significantly modified the number of GnRH pulses (Figure 8, sequential control: 6.3 ± 0.309 pulses; sequential experimental: 1.7 ± 0.555 pulses, $p < 0.05$). ZD7288 significantly impacted the average IPI, when compared to the first 120 minutes of Locke's medium (Figure 9, contrast control: 19.5 ± 1.20 minutes; contrast experimental: 26.4 ± 1.31 minutes; $p < 0.05$). The variation in average IPI and pulse peak values between the control and experimental groups, when compared to the sequential groups, can be associated with the shortened timeframes of the sequential control and sequential experimental exposures.

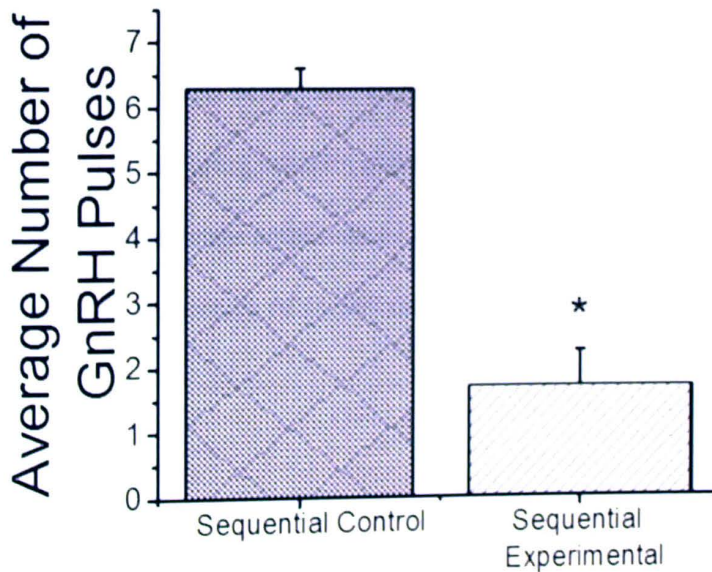


Figure 8: The average number of GnRH pulses detected by Dynpeak, before and after exposure to ZD7288. The decrease in pulse peaks detected after exposure to ZD7288 is statistically significant (Sequential Control: 6.33 ± 0.309 pulses, $n=12$; Sequential Experimental: 1.667 ± 0.555 pulses, $n=12$, $p < 0.05$).

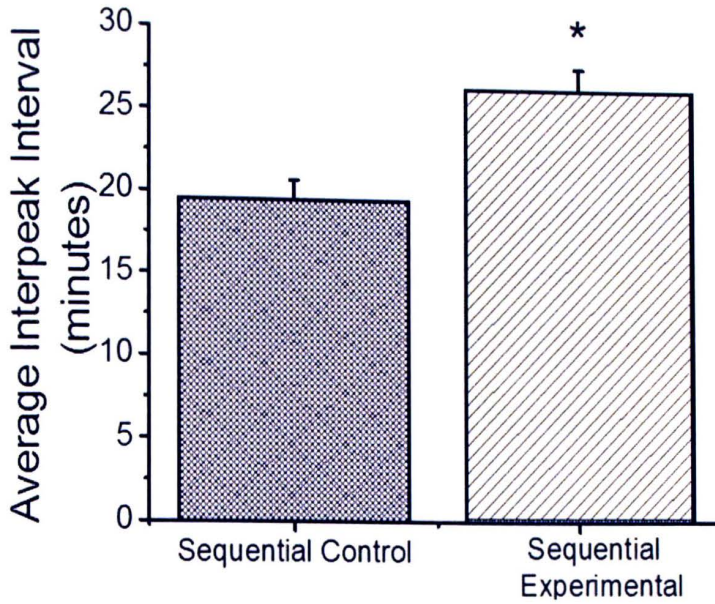


Figure 9: Bar graph depiction of the mean number of interpeak intervals, recorded in minutes, detected by Dynpeak, before and after exposure to ZD7288. The increase in interpeak intervals detected after exposure to ZD7288 is statistically significant (Sequential Control: 19.6 ± 1.265 minutes, $n=12$; Sequential Experimental: 26.4 ± 1.671 minutes, $n=12$, $p < 0.05$).

To better present the effects before and after ZD7288 exposure, Figure 10 depicts a typical profile of GnRH levels during medium control perfusion. Eight GnRH pulses are identified in panel A with an average amplitude of 41,500 ng/ml. Panel B shows the interpeak intervals which occurred at an average of 16.667 minutes between pulse peaks.

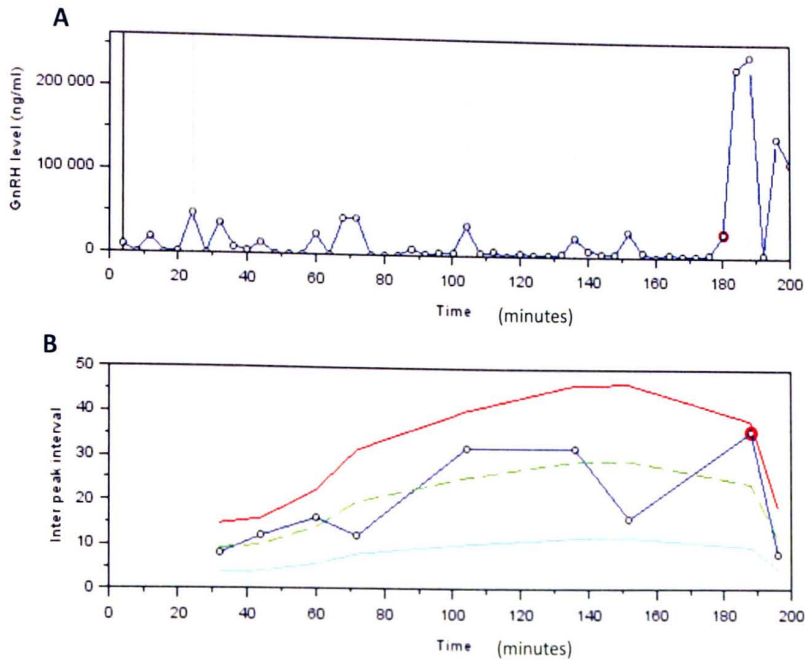


Figure 10: Control culture receiving only Locke's medium for 180 minutes. At 180th minute veratridine was added to determine cell viability. Panel A: 8 pulse peaks recorded at an average of 41,500 ng/ml. Panel B: Interpeak intervals recorded at an average of 16.667 minutes between pulse peaks.

Figure 11 depicts a typical profile of GnRH levels during continuous ZD7288 exposure. Seven GnRH pulses are depicted in panel A with an average amplitude of 3,400 ng/ml. Panel B shows the average interpeak intervals which averaged 21.429 minutes between pulse peaks. IPI measurements are estimated after 70 minutes into perfusion because of a latency period, lacking true GnRH pulse peaks. After 70 minutes of ZD7288 exposure, pulse peaks are regularly recorded and IPI can be measured.

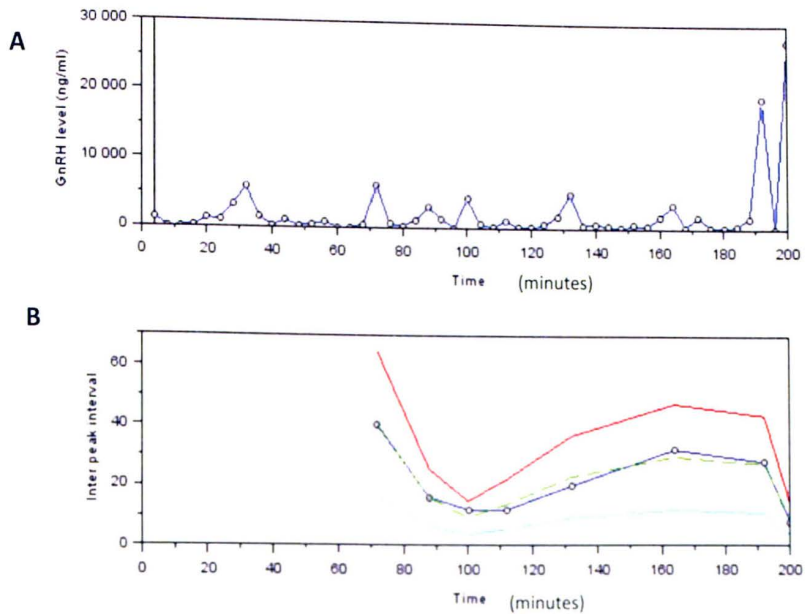


Figure 11: Experimental culture 1 receiving 50 μ M zd7288 dissolved in Locke's medium for 180 minutes. At 180th minute veratridine was added to determine cell viability. Panel A: 7 pulse peaks recorded at an average 3,400 ug/ml. Panel B: Interpeak intervals recorded at an average of 21.429 minutes between pulse peaks.

Figure 12 depicts the typical profile of GnRH levels before (0-120 minutes) and during application of ZD7288 (120-240 minutes) to GT1-7 cells. Panel A depicts six GnRH peaks during the sequential control period with an average amplitude of 66,700 ng/ml and three GnRH peaks with an average amplitude of 1,800 ng/ml during ZD7288 perfusion. Panel B shows the average interpeak intervals which averaged 20 minutes before the application of ZD7288 and 27.5 minutes after addition of ZD7288. Veratridine response is low, assumedly from ZD7288 exposure, lacking wash-out. There was still a recorded response to veratridine and the cells are assumed to have survived the experimental procedure.

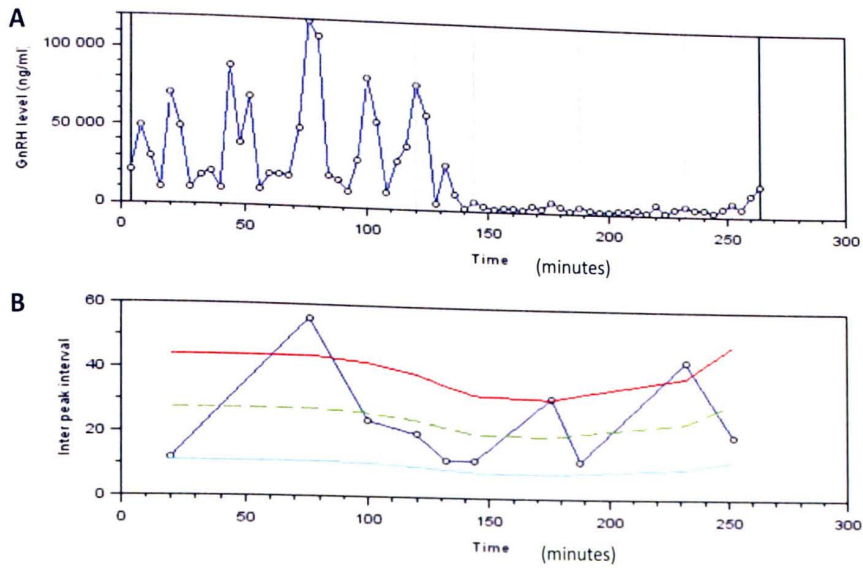


Figure 12: Sequential culture receiving Locke's medium for 120 minutes, then treated with 50 μ M ZD7288 dissolved in Locke's medium for 120 minutes. At 240th minute veratridine was added to determine cell viability. Panel A: 6 pulse peaks recorded at an average 66,700 ug/ml. Panel B: Interpeak intervals recorded at an average of 20 minutes between pulse peaks. Panel A: 3 pulse peaks were detected at an average of 1,800 ug/ml, with an interpeak interval of 27.5 minutes after addition of ZD7288 (Panel B).

Table 1 compares the average number of GnRH pulses that were identified during the first 120 minutes and the second 120 minutes of all perfusions. There was not significant difference in the number of GnRH pulses during either period in which Locke's medium was continuously perfused (control 1 vs. control 2). In addition, there was no significant difference in the number of GnRH pulses during the first 120 minutes of the continuous Locke's perfusion or the sequential control period (Control 1 vs. Sequential Control). In contrast, the numbers of GnRH pulses were significantly different when the control periods were compared to the sequential experimental period ($p < 0.05$).

Treatment Comparison	Average number of pulse peaks (mean +/- SEM)	Average number of pulse peaks (mean +/- SEM)
Control 1 vs. Control 2	4.33 +/- 0.10	4.67 +/- 0.10
Control 1 vs Sequential Control	4.33 +/- 0.10	6.33 +/- 0.31
Sequential Control vs Sequential Experimental*	6.33 +/- 0.31	1.67 +/- 0.55
Control 2 vs Sequential Experimental*	4.67 +/- 0.10	1.67 +/- 0.55
Experimental 2 vs Control 2	3.3 +/- 0.19	4.67 +/- 0.10
Experimental 2 vs Sequential Experimental	3.3 +/- 0.19	1.67 +/- 0.55

Table 1: The average number of GnRH pulses (mean +/- SEM). Control 1 (n=12) measurements from 0-120 minutes perfusion with Locke's medium. Control 2 (n=12) measurements from 120-240 minutes perfusion with Locke's medium. Sequential Control (n=12) measurements from 0-120 minutes perfusion with Locke's medium. Sequential Experimental (n=12) measurements from 120-240 minutes perfusion with ZD7288 dissolved in Locke's medium. There is a statistically significant difference (*) between the Sequential Control vs. Sequential Experimental, and between Control 2 vs. Sequential Experimental. $p < 0.05$.

Table 2 compares the average interpeak intervals, recorded in minutes, which were identified during the first 120 minutes and the second 120 minutes of all perfusions. There was not significant difference in the average IPI's during either period in which Locke's medium was continuously perfused (control 1 vs. control 2). In addition, there was no significant difference in

the average IPI's during the first 120 minutes of the continuous Locke's perfusion or the sequential control period (Control 1 vs. Sequential Control). In contrast, the IPI's were significantly different when the control periods were compared to the sequential experimental period and the experimental 2 period ($p<0.05$).

Treatment Comparison	Average interpeak intervals (minutes, mean +/- SEM)	Average interpeak intervals (minutes, mean +/- SEM)
Control 1 vs. Control 2	18.67+/-0.075	17.81 +/- 0.98
Control 1 vs Sequential Control	18.67+/-0.07	19.56+/-1.67
Sequential Control vs Sequential Experimental*	19.56+/-1.67	26.43+/-1.67
Control 2 vs Sequential Experimental*	17.81 +/- 0.98	26.43+/-1.67
Experimental 2 vs Control 2*	24.13 +/- 1.199	17.81 +/- 0.98
Experimental 2 vs Sequential Experimental	24.13 +/- 1.199	26.43 +/- 1.67

Table 2: Average GnRH interpeak interval (minutes, mean +/- SEM). Control 1 (n=12) measurements from 0-120 minutes perfusion with Locke's medium. Control 2 (n=12) measurements from 120-240 minutes perfusion with Locke's medium. Sequential Control (n=12) measurements from 0-120 minutes perfusion with Locke's medium. Sequential Experimental (n=12) measurements from 120-240 minutes perfusion with ZD7288 dissolved in Locke's medium. There is a statistically significant difference (*) between the Sequential Control vs. Sequential Experimental, Experimental 2 vs Control 2, and between Control 2 vs. Sequential Experimental. $p<0.05$.

Statistical analysis supports a significant difference in the number of GnRH peaks produced by both the experimental cultures and sequential experimental cultures, when compared to the number of pulse peaks within both the control cultures and sequential control cultures (Figure 6 and 8; Table 1, $p < 0.05$). In addition, the average IPI and Frequency of pulses per hour was altered after exposure to ZD7288, (Figure 7, 9, and 14; Table 2, $p < 0.05$). Finally, the average amplitudes of the GnRH pulses decreases ± 10 fold after exposure to ZD7288 (Figures 10, 11, 12 and 13).

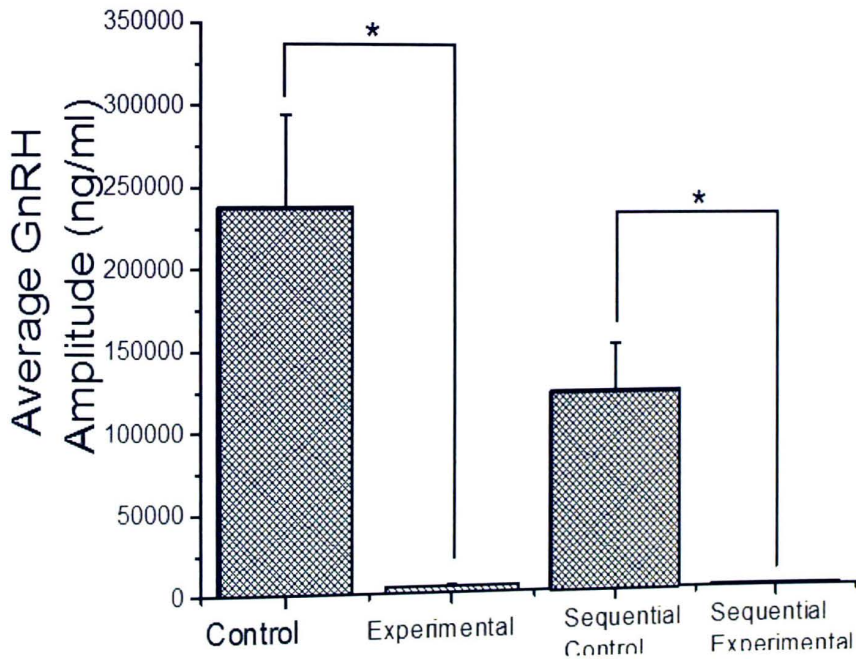


Figure 13: The average GnRH pulse amplitudes during the control and experimental groups. ZD7288 significantly altered the amplitude of GnRH peaks (Control: 237,917 \pm 57010.2939 ng/ml Experimental: 4,600 \pm 319.03 μ g/ml Sequential Control: 123,333 \pm 29215.32737 ng/ml Sequential Experimental: 1,000 \pm 426.4014327 ng/ml. $p < 0.05$).

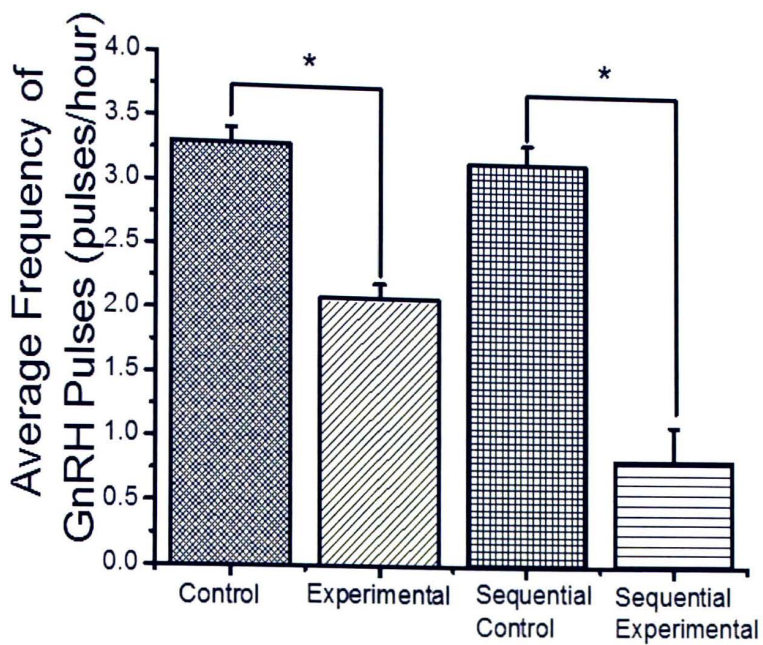


Figure 14: The average frequency of GnRH pulses (pulse/hr \pm SEM).
(Control: 3.32/hr \pm 0.119; Experimental: 2.2/hr \pm 0.112; Sequential Control: 3.2/hr \pm 0.155; Sequential Experimental: 0.833/hr \pm 0.278. $p < 0.05$)

CHAPTER V: Discussion

Hyperpolarizing events and episodic hormonal release seem to be principal attributes of GnRH neurons (De Escalera *et al.*, 1992; Mellon *et al.*, 1990). In our study, the obstruction of hyperpolarization-activated cation channels by ZD7288 altered the number of GnRH pulses, effected the average pulse amplitude, altered pulse frequency, and altered the average interpeak intervals. To examine HCN channels as a possible factor in controlling and synchronizing GnRH secretions, this study utilized GT1-7 cells, a line of immortalized cells derived from transgenic mice carrying a GnRH promoter-driven oncogene (Mellon *et al.*, 1990). These cells express HCN channels and are observed to produce synchronized pulses of GnRH. ZD7288, a known HCN channel blocker (Luo *et al.*, 2007) was applied to GT1-7 cells to examine the role of HCN in the control of GnRH secretion.

GT1-7 cells, an immortalized line of GnRH neurons, were chosen as a model system to determine the effects of ZD7288 on GnRH secretion because GT1-7 cells are completely isolated without contamination of other types of cells, so observations of direct effects can be made. These cells display the biophysical properties expected of GnRH neurons, including rhythmic action potentials and episodic secretion of GnRH (Mellon *et al.*, 1990). The capacity of GT1 cells to display periodic GnRH discharge without the influence of other cell types, provides an excellent model to study the effect of HCN channel blockers on pulsatile GnRH discharge (Funahashi *et al.*, 2003).

Cell viability was examined at the end of each experiment through the addition of veratridine to the perfusion medium (De Escalera *et al.*, 1992). Veratridine prevents Na^+

channels from closing, thus depolarizing intact cells and causing the release of synaptic vesicles (De Escalera *et al.*, 1992). Veratridine has been used in several studies to demonstrate cell viability (De Escalera *et al.*, 1992). Therefore, it is unlikely that the change in GnRH pulse frequency and amplitude was due to a reduction in GT1-7 cell viability.

To examine the direct effects of ZD7288 on GnRH secretion, we used three treatment groups (Figure 4). The first was a control treatment group for gathering the baseline controls of normal GnRH secretion produced by GT1-7 cells. The second was an experimental treatment, to gather the effects of continuous ZD7288 exposure and the resulting effects on GnRH secretion. The third and arguably the most important, was the sequential treatment group, where ZD7288 was added mid-treatment, in order to analyze the effects of ZD7288, with a direct comparison of a normal GT1-7 GnRH secretions. This provided an image that allowed us to verify the effect of ZD7288, while ensuring the change in GnRH secretions were not a result of error or noise (Figure 6, 7, 8, 9, 13, and 14; Table 1 and 2).

ZD7288 has been proven to block HCN channels, and I_h , which in turn, alters GnRH neuronal activity (Chu *et al.*, 2010; Wu *et al.*, 2012). Schauer *et al.*, (2015) showed that GnRH neuronal activity directly correlated with the modulation of the estrous cycle of female mice. The decrease of pulse amplitude and frequency in the current study compliments the results of Chu *et al.*, (2010) and Schauer *et al.*, (2015). Chu *et al.*, (2010), which reported decreased GnRH neuronal excitability when ZD7288 was added to GnRH neurons from castrated male mice gives support and validation to our finding that show a change in GnRH secretions after administration of ZD7288. During exposure to ZD7288, there was a decrease in I_h and HCN activation (Chu *et al.*, 2010), from this, combined with the findings of Schauer *et al.*, (2015), one could infer that the changes in GnRH we recorded after ZD7288 administration was due to a decrease in

neuronal activity of the GT1-7 cells. Furthermore, voltage dependence of HCN channels are effected by hormones, making them easily effected by extracellular environments (Chu *et al.*, 2010). Modulation of HCN activation may be the mechanism by which estradiol or KISSPEPTIN mediate GnRH secretion, this requires further investigation.

There are a few points that require future investigation, one is the research by Constantin S. and Wray S. (2008). This study shows that, GnRH-1 neuronal activity is independent of HCN channels. Furthermore, the research showed that neuronal activity of GnRH-1 neurons was facilitated through cAMP-dependent activation of protein kinase A-dependent phosphorylation (PKA) (Constantin S. and Wray S. 2008). Calcium imaging of nasal explant GnRH-1 neuronal activity, after ZD7288 administration still showed cyclic oscillatory electrical activity, suggesting that HCN channels are not necessary for synchronization. It would be necessary to re-examine these findings, in combination with GnRH hormonal measurements.

Another area for future research which our present study does not include, is castration, which was mentioned in the study of Chu *et al.*, (2010). Castration was seen to expand GnRH action potential frequency and increased the amplitude of I_h in GnRH neurons (Chu *et al.*, 2010). In males there is generous amounts of estradiol in the cerebrum, transformed from testosterone from the gonads, which gives the essential negative feedback signal to decrease the GnRH and GnRH-subordinate discharge of gonadotropins from the pituitary. Treatment of castrated male mice with estradiol reestablished I_h to levels observed in gonadal intact mice, suggesting that estradiol mediated changes in I_h are a part of this negative input component. Since ZD7288 is a known HCN channel blocker and is shown to block I_h , this suggests that estradiol is mediating effects through modulation of HCN channels (Chu *et al.*, 2010). Regardless of whether feedback

mechanism directly influences HCN activity or has a secondary effector, remains to be resolved (Chu *et al.*, 2010).

Lastly, the present study also does not deal with the role of kisspeptins and its association with GnRH neurons. Kisspeptin (Kiss1) neurons are known to elicit some positive-feedback mechanisms associated with GnRH secretions (Zhang *et al.*, 2013; Chappell *et al.*, 2000). GnRH neurons express the kisspeptin receptor, GPR 54, and kisspeptins intensely fortify the arrival of GnRH by depolarizing and stimulating activity potential terminating in GnRH neurons (Zhang *et al.*, 2013). Accordingly, Kiss1 neurons might be the pre-synaptic pacemaker neurons in the hypothalamic hardware that controls excitation and secretion. There are no less than two distinct populaces of Kiss1 neurons: one in the rostral periventricular territory (RP3V) that is positively mediated by estrogens and the other in the arcuate core that react to the negative feedback from estrogens (Zhang *et al.*, 2013; Chappell *et al.*, 2000). How each of these Kiss1 neuronal populaces provide a role in controlling of the GnRH cycle is an area of active research.

In conclusion, our results demonstrate that GnRH secretion is effected by the HCN channel blocker ZD7288, *in-vitro*. It can therefore be inferred that HCN channels have an effect in modulating GnRH secretion, although further investigation is required. HCN channels are effected by hormonal inputs, and would provide a good explanation for the neuronal capabilities of GnRH cells to produce episodic action potentials in isolated cell cultures, while supporting the regulatory effect of E2 and conductances from kisspeptin neurons. This research provides novel insight into the connections between cellular electrical activities and their role in effecting major cellular functions. This provides further insights to understanding the integral components which effect the neuroendocrine axes, and thus, controlling main physiological functions such as growth, development, and reproduction.

CHAPTER VI: References

- Altomare C., Terragni B., Brioschi C. (2003). Heteromeric HCN1–HCN4 channels: a comparison with native pacemaker channels from the rabbit sinoatrial node. *Journal of Physiology*, 549:347–359.
- Aponte, Y., Lien, C.C., Reisinger, E., & Jonas, P. (2006). Hyperpolarization-activated cation channels in fast-spiking interneurons of rat hippocampus. *Journal of Physiology*, 574 (1), 229-243.
- Arroyo, A., Kim, B., Rasmusson, R. L., Bett, G., & Yeh, J. (2006). Hyperpolarization-activated cation channels are expressed in rat hypothalamic gonadotropin-releasing hormone (GnRH) neurons and immortalized GnRH neurons. *Journal of the Society for Gynecologic Investigation*, 13(6), 442-450.
- Biel, M., Ludwig, A., Zong, X., & Hofmann, F. (1999). Hyperpolarization-activated cation channels: a multi-gene family. In *Reviews of Physiology, Biochemistry and Pharmacology, Volume*, 136:165-181.
- Biel M., Wahl-Schott C., Stylianos M. (2009). Hyperpolarization-activated cation channels: from genes to function. *Physiol Rev*, 89:847–885
- Brown, H.F., D. DiFrancesco, S.J. Noble. (1979). How does adrenaline accelerate the heart? *Nature*, 280:235–236.
- Clarke, I.J., & Cummins, J.T. (1985). GnRH pulse frequency determines LH pulse amplitude by altering the amount of releasable LH in the pituitary glands of ewes. *Journal of Reproductive Fertility*, 73: 425-431.
- Chappell P.E., Levine J.E. (2000). Stimulation of gonadotropin-releasing hormone surges by estrogen. I Role of hypothalamic progesterone receptors. *Endocrinology*, 141:1477–1485

Chen, X., Iremonger, K., Herbison, A., Kirk, V., Sneyd, J. (2013). Regulation of electrical bursting in a spatiotemporal model of a GnRH neuron. *Bulletin of mathematical biology*, 75(10): 1941-1960.

Chu, Z., & Moenter, S. M. (2006). Physiologic regulation of a tetrodotoxin-sensitive sodium influx that mediates a slow after depolarization potential in gonadotropin-releasing hormone neurons: possible implications for the central regulation of fertility. *The Journal of Neuroscience*, 26(46): 11961-11973.

Chu, Z., Takagi, H., & Moenter, S. M. (2010). Hyperpolarization-activated currents in gonadotropin-releasing hormone (GnRH) neurons contribute to intrinsic excitability and are regulated by gonadal steroid feedback. *The Journal of Neuroscience*, 30(40): 13373-13383.

Clarençon, D., Renaudin, M., Gourmelon, P., Kerckhoeve, A., Catérini, R., Boivin, E., & Fatôme, M. (1996). Real-time spike detection in EEG signals using the wavelet transform and a dedicated digital signal processor card. *Journal of neuroscience methods*, 70(1): 5-14.

Constantin S., Wray S. (2008). Gonadotropin-releasing hormone-1 neuronal activity is independent of cyclic nucleotide-gated channels. *Endocrinology*. 149(1):279-90.

DiFrancesco D. (1981). A study of the ionic nature of the pace-maker current in calf Purkinje fibres. *Journal of Physiology*, 314:377-393.

DeFazio, R. A., & Moenter, S. M. (2002). Estradiol feedback alters potassium currents and firing properties of gonadotropin-releasing hormone neurons. *Molecular Endocrinology*, 16(10): 2255-2265.

De La Escalera, G. M., Choi, A. L., & Weiner, R. I. (1992). Generation and synchronization of gonadotropin-releasing hormone (GnRH) pulses: intrinsic properties of the GT1-1 GnRH neuronal cell line. *Proceedings of the National Academy of Sciences*, 89(5): 1852-1855.

- Eisthen, H.L., Delay, R.J., Wirsig-Wiechmann, C.R., & Dionne, V.E. (2000). Neuromodulatory Effects of Gonadotropin Releasing Hormone on Olfactory Receptor Neurons. *The Journal of Neuroscience*, 20(11): 3947-3955.
- Emery E., Young G., McNaughton P. (2012). HCN2 ion channels: an emerging role as the pacemakers of pain. *Trends in Pharmacological Sciences*, 33(8): 456–463.
- Farsian M. and Pitts G. (2008). Luteinizing Hormone Releasing Hormone Assaying: Optimization of an Enzyme Immunoassay for the Detection of Gonadotropin-releasing Hormone. Thesis. Austin Peay State University.
- Funahashi, M., Mitoh, Y., Kohjitani, A., & Matsuo, R. (2003). Role of the hyperpolarization activated cation current (I_h) in pacemaker activity in area postrema neurons of rat brain slices. *Journal of Physiology*, 552(1): 135-148.
- Hall, J., Lavoie, H., Marsh, E., Martin, K. (2000). Decrease in Gonadotropin-Releasing Hormone (GnRH) Pulse Frequency with Aging in Postmenopausal Women. *Journal of Clinical Endocrinology Metabolism*, 85(5): 1794-1800.
- Han S.K., Gottsch M.L., Lee K.J., Popa S.M., Smith J.T., Jakawich S.K., Clifton D.K., Steiner R.A., Herbison A.E. (2005). Activation of gonadotropin-releasing hormone neurons by kisspeptin as a neuroendocrine switch for the onset of puberty. *The Journal of Neuroscience*, 25:11349–11356.
- Jacob, D. A., Temple, J. L., Patisaul, H. B., Young, L. J. & Rissman, E. F. 2001. Coumestrol Antagonizes Neuroendocrine Actions of Estrogen via the Estrogen Receptor α . *Exp Biol Med*, 226, 301.
- Jayes F.C., Britt J.H., Esbenshade K.L. (1997). Role of gonadotropin-releasing hormone pulse frequency in differential regulation of gonadotropins in the gilt. *Biology of Reproduction*, 56 (4): 1012–9.
- Kato, M., Ui-Tei, K., Watanabe, M., & Sakuma, Y. (2003). Characterization of voltage-gated calcium currents in gonadotropin-releasing hormone neurons tagged with green fluorescent protein in rats. *Endocrinology*, 144(11): 5118-5125.

Keenan, D. M., Clarke, I. J., & Veldhuis, J. D. (2011). Noninvasive analytical estimation of endogenous GnRH drive: analysis using graded competitive GnRH-receptor antagonism and a calibrating pulse of exogenous GnRH. *Endocrinology*, 152(12): 4882-4893.

Kelly, M. J., Zhang, C., Qiu, J., & Rønnekleiv, O. K. (2013). Pacemaking kisspeptin neurons. *Experimental physiology*, 98(11), 1535-1543.

Kranig, S. A., Duhme, N., Waldeck, C., Draguhn, A., Reichinnek, S., & Both, M. (2013). Different functions of hyperpolarization-activated cation channels for hippocampal sharp waves and ripples in vitro. *Neuroscience*, 228:325-333.

Kuehl-Kovarik M.C., Pouliot W.A., Halterman G.L., Handa R.J., Dudek F.E., Partin K.M. (2002). Episodic bursting activity and response to excitatory amino acids in acutely dissociated gonadotropin-releasing hormone neurons genetically targeted with green fluorescent protein. *Journal of Neuroscience*, 22:2313–2322.

Lacau-Mengido, I. M., Iglesias, A. G., Díaz-Torga, G., Thyssen-Cano, S., Libertun, C., & Becú-Villalobos, D. (1998). Effect of stage of development and sex on gonadotropin-releasing hormone secretion in in vitro hypothalamic perfusion. *Experimental Biology and Medicine*, 217(4): 445-449.

Luo L, Chang L, Brown SM, Ao H, Lee DH, Higuera ES.. (2006). Role of peripheral hyperpolarization-activated cyclic nucleotide-modulated channel pacemaker channels in acute and chronic pain models in the rat. *The Journal of Neuroscience*, 144:1477–85.

McCormick, D. A., & Pape, H. C. (1990). Properties of a hyperpolarization-activated cation current and its role in rhythmic oscillation in thalamic relay neurones. *The Journal of physiology*, 431: 291.

Mellon, P. L., Windle, J. J., Goldsmith, P. C., Padula, C. A., Roberts, J. L., & Weiner, R. I. (1990). immortalization of hypothalamic GnRH by genetically targeted tumorigenesis. *Neuron*, 5(1): 1-10.

- Messenger S., Chatzidaki E., Ma D., Hendrick G., Zahn D., Dixon J., Thresher R., Malinge I., Lomet D., Carlton M.B. (2005). Kisspeptin directly stimulates gonadotropin-releasing hormone release via G protein-coupled receptor 54. *Proc. Natl. Acad. Sci. USA*. 5:1761–1766.
- Moenter, S. M., Brand, R. C., & Karsch, F. J. (1992). Dynamics of gonadotropin-releasing hormone (GnRH) secretion during the GnRH surge: insights into the mechanism of GnRH surge induction. *Endocrinology*, 130(5): 2978-2984.
- Nunemaker, C. S., Straume, M., DeFazio, R. A., & Moenter, S. M. (2003). Gonadotropin-releasing hormone neurons generate interacting rhythms in multiple time domains. *Endocrinology*, 144(3), 823-831.
- Piet, R., Boehm, U., & Herbison, A. E. (2013). Estrous cycle plasticity in the hyperpolarization-activated current ih is mediated by circulating 17 β -estradiol in preoptic area kisspeptin neurons. *The Journal of Neuroscience*, 33(26), 10828-10839
- Roseweir K., Kauffman S., Smith T., Guerriero A., Morgan K., Pielecka-Fortuna J., Pineda R., Gottsch L., Tena-Sempere M., Moenter S. (2009). Discovery of potent kisspeptin antagonists delineate physiological mechanisms of gonadotropin regulation. *Journal of Neuroscience*, 12:3920–3929.
- Ruka, K. A. (2015). *Neuropeptide and Gonadal Steroid Action on Arcuate Kisspeptin Neurons: Implications for Central Regulation of Fertility* (Doctoral dissertation, University of Michigan).
- Schally, A. V., Arimura, A., Kastin, A. J., Matsuo, H., Baba, Y., Redding, T. W., & White, W. F. (1971). Gonadotropin-releasing hormone: one polypeptide regulates secretion of luteinizing and follicle-stimulating hormones. *Science*, 173(4001): 1036-1038.
- Schauer C., Tong T., Petitjean H., Blum T., Peron S., Mai O., Schmitz F., Boehm U., Leinders-Zufall T. (2015). Hypothalamic gonadotropin-releasing hormone (GnRH)

receptor neurons fire in synchrony with the female reproductive cycle. *Journal of Neurophysiology*, 114(2): 1008-10021.

Sliwowska J. H., Fergani C., Gawalek M., Skowronska B., Fichna P., Lehman M. N. (2014). Insulin: its Role in the Central Control of Reproduction. *Physiology and Behavior*, 0: 197–206.

Silverman, A. J. (1988). *The Physiology of Reproduction*, eds. Knobil, E. & Neill, J. D. (Raven, New York), pp. 1283-1304.

Smith T., Popa M., Clifton K., Hoffman E., Steiner A. (2006). Kiss1 neurons in the forebrain as central processors for generating the preovulatory luteinizing hormone surge. *Journal of Neuroscience*, 25:6687–6694.

Thompson E.L., Patterson M., Murphy K.G., Smith K.L., Dhillon W.S., Todd J.F., Ghatei M.A., Bloom S.R. (2004). Central and peripheral administration of kisspeptin-10 stimulates the hypothalamic-pituitary-gonadal axis. *Journal of Neuroendocrinology*, 10:850–858.

Vidal, E., Zhang, Q., Me'sigue, C., Fabre, S., Clement, F. (2012). DynPeak: An Algorithm for Pulse Detection and Frequency Analysis in Hormonal Time Series. *PLoS ONE*, 7 (7): 1-16.

Wu, X., Liao, L., Liu, X., Luo, F., Yang, T. & Li, C. (2012). Is ZD7288 a selective blocker of hyperpolarization activated cyclic nucleotide-gated channel currents? *Channels*, 6 (6):1-5.

Wen, J. P., Lv, W. S., Yang, J., Nie, A. F., Cheng, X. B., Yang, Y., & Ning, G. (2008). Globular adiponectin inhibits GnRH secretion from GT1-7 hypothalamic GnRH neurons by induction of hyperpolarization of membrane potential. *Biochemical and biophysical research communications*, 371(4): 756-761.

Yu, X., Duan, K.L., Shang, C.F., Yu, H.G., & Z.Z. (2004). Calcium influx through hyperpolarization-activated cation channels (Ih channels) contributes to activity-evoked neuronal secretion. *PNAS*, 101 (4): 1051-1056.

Yu X., Duan K.L., Shang C.F., (2004). Calcium influx through hyperpolarization-activated cation channels [I(h) channels] contributes to activity-evoked neuronal secretion. *Proc. Natl. Acad. Sci. U.S.A.*, 101:1051–1056.

Zhang C., Tonsfeldt K.J., Qiu J., Bosch M.A., Kobayashi K., Steiner R.A., Kelly M.J., Rønnekleiv O.K. (2013). Molecular mechanisms that drive estradiol-dependent burst firing of Kiss1 neurons in the rostral periventricular preoptic area. *American Journal of Physiology Endocrinology Metabolism*. 305: E1384–E1397.

APPENDIX A: Pulse Analysis for Control Cells

This appendix contains figures which depict the amount of GnRH secreted by GT1-7 cell cultures that were perfused with Locke's medium for 180 minutes. In each figure, Panel A depicts the amount of GnRH secreted during each 4-minute collection period. "True" pulse peaks were determined by the Dynpeak analysis software and are denoted by vertical lines. Panel B is part of the Dynpeak output and shows the true IPI values in blue and corresponds to the duration of time between each pulse peak recorded. The dashed green lines indicate the moving cubic function fitting the values of the IPI series. The lower and upper solid lines indicate the edges of the GnRH tunnel, indicating the normal ranges of pulse peaks expected throughout each series. Unusually high or low pulse peaks are indicated by their occurrence outside of the GnRH tunnel, and indicate the possibility of pulse outliers. Unusually high pulse peaks, outside of the tunnel, could suggest that there were multiple 'true' GnRH secretory events that occurred in a short time frame, and results in one large pulse peak being detected. Pulse peaks occurring below the tunnel, signifies a low probability of a true secretory event. GnRH pulses that fell outside GnRH tunnel were not counted as pulse. Peaks after veratridine exposure were not included, but noted for cell viability.

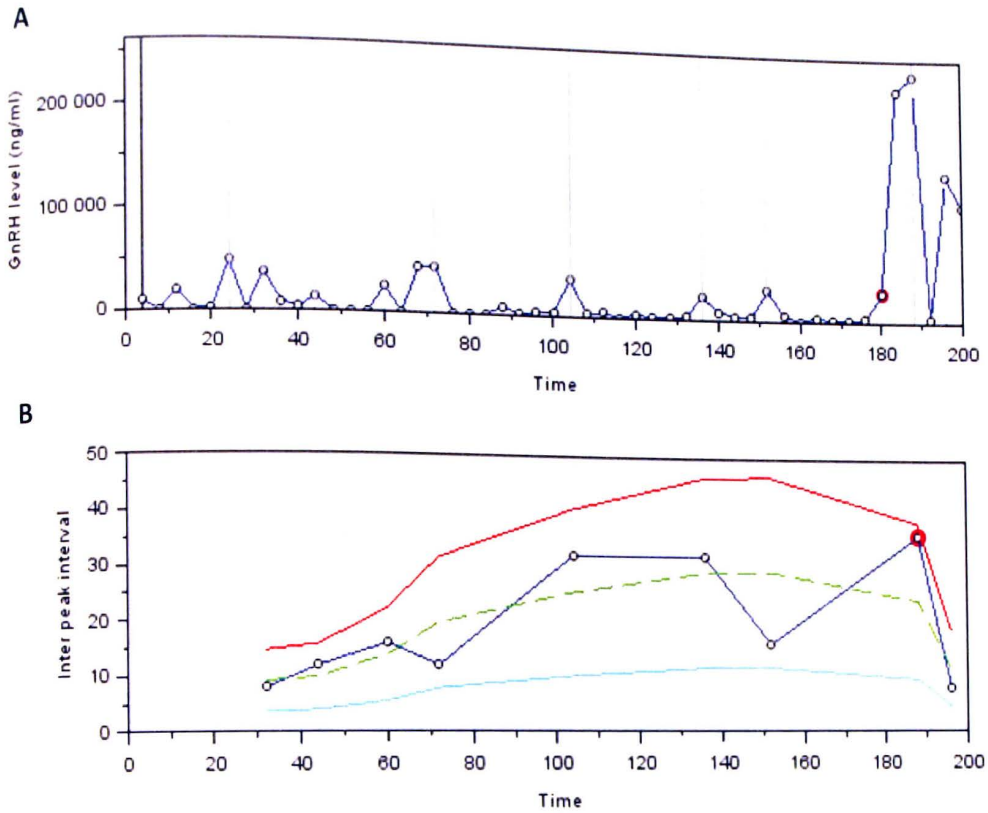


Figure 1: Control culture 1 receiving only Locke's medium for 180 minutes. At 180th minute veratridine was added to determine cell viability. Panel A: 8 pulse peaks recorded at an average 50,000 ng/ml. Panel B: Interpeak intervals recorded at an average of 16.667 minutes between pulse peaks.

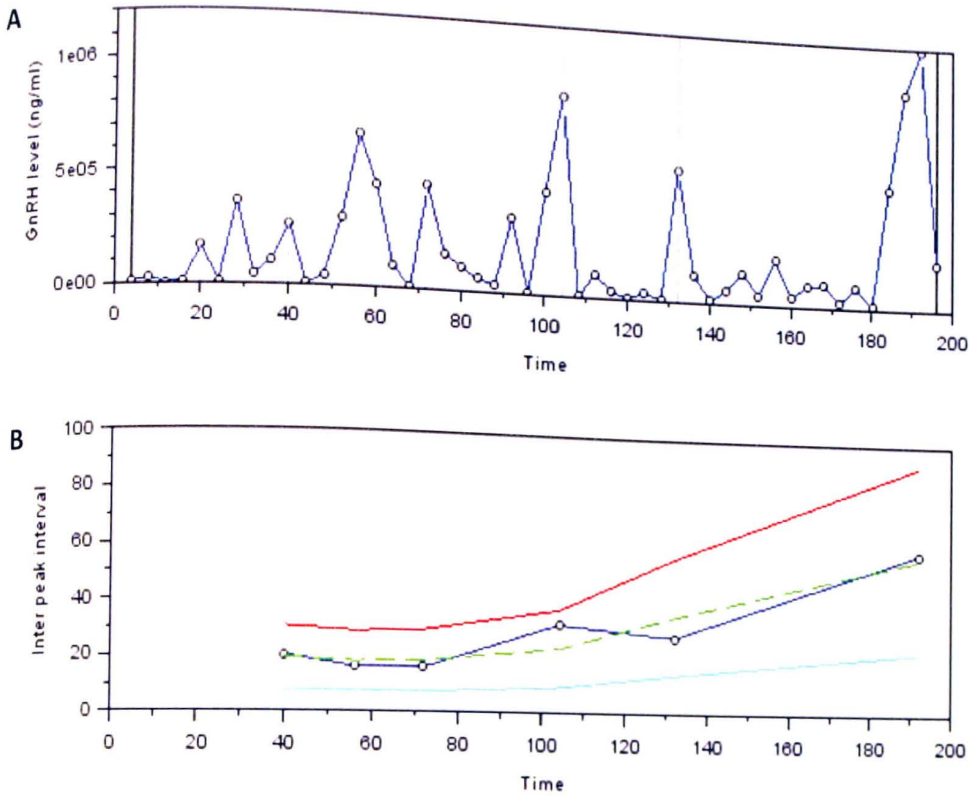


Figure 2: Control culture 2 receiving only Locke's medium for 180 minutes. At 180th minute veratridine was added to determine cell viability. Panel A: 6 pulse peaks recorded at an average 250,000 ng/mL. Panel B: Interpeak intervals recorded at an average of 25.83 minutes between pulse peaks.

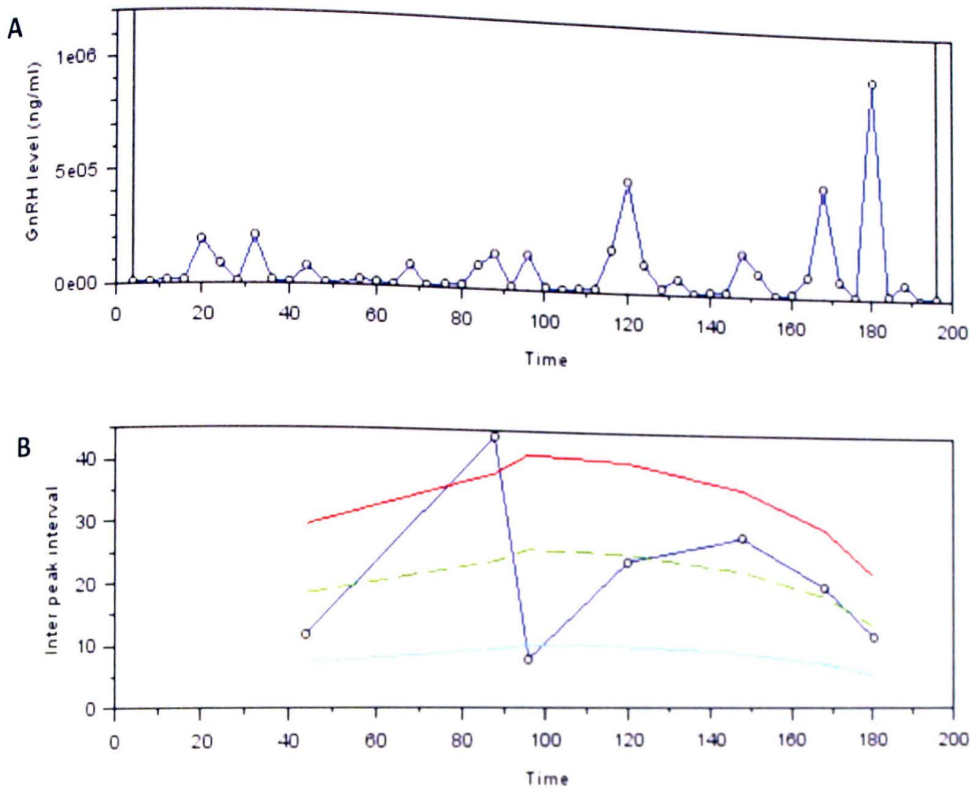


Figure 3: Control culture 3 receiving only Locke's medium for 180 minutes. At 180th minute veratridine was added to determine cell viability. Panel A: 7 pulse peaks recorded at an average 250,000 ng/mL. Panel B: Interpeak intervals recorded at an average of 17.143 minutes between pulse peaks.

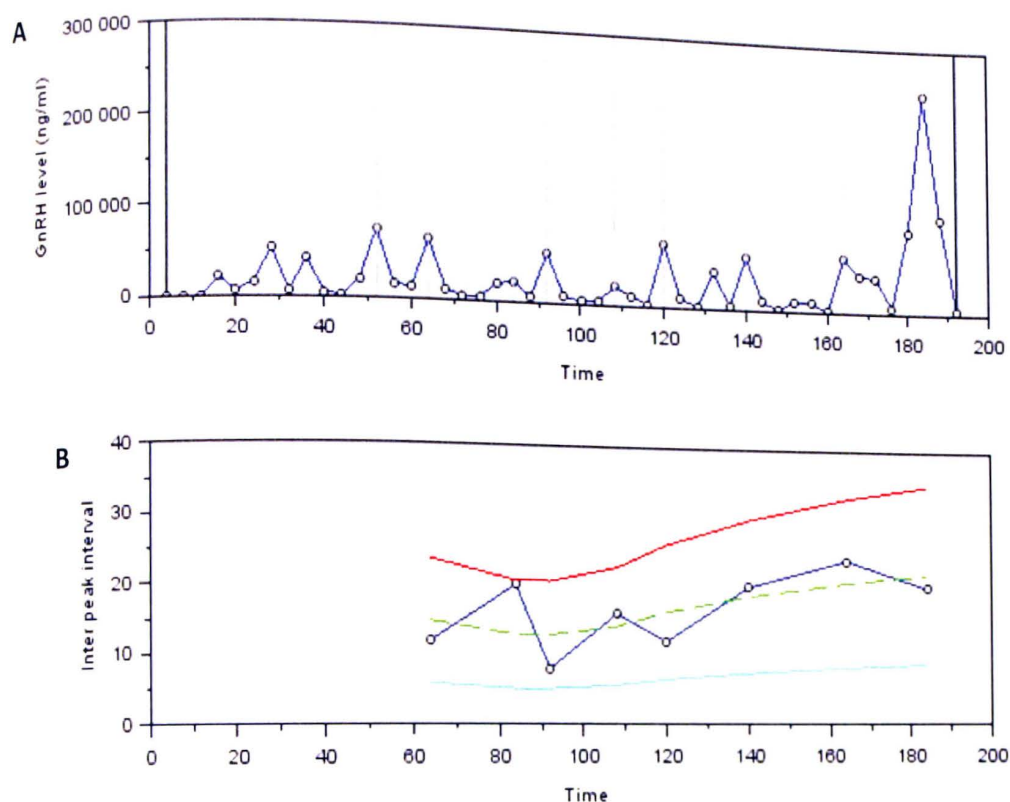


Figure 4: Control culture 4 receiving only Locke's medium for 180 minutes. At 180th minute veratridine was added to determine cell viability. Panel A: 8 pulse peaks recorded at an average 80,000 ng/mL. Panel B: Interpeak intervals recorded at an average of 13.75 minutes between pulse peaks.

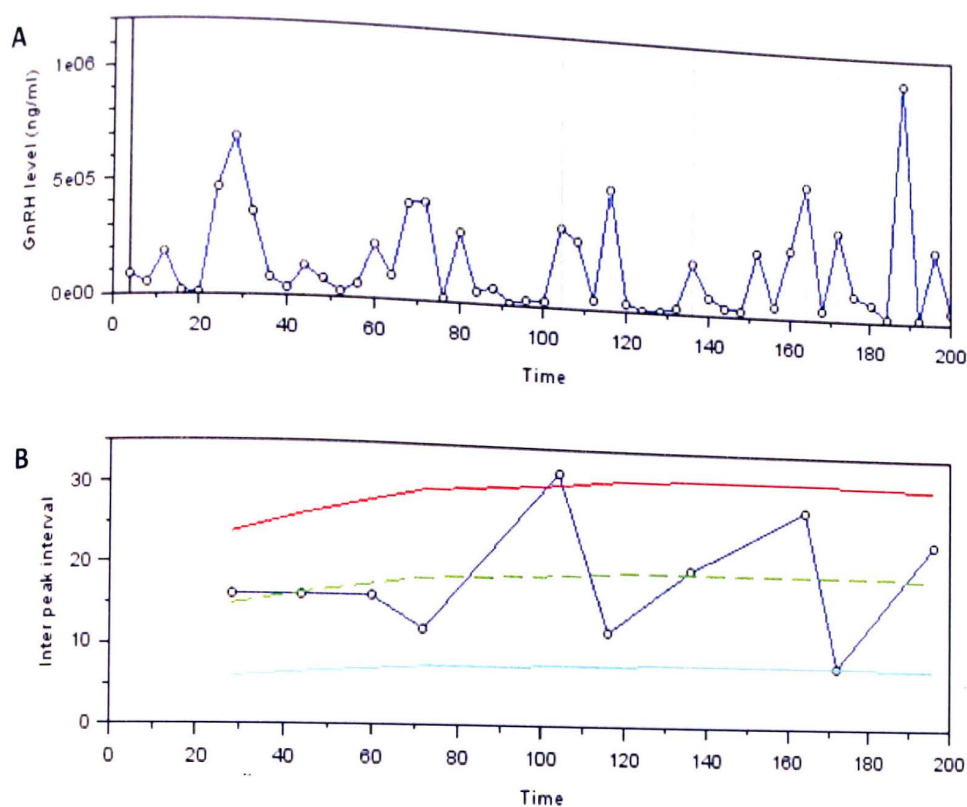


Figure 5: Control culture 5 receiving only Locke's medium for 180 minutes. At 180th minute veratridine was added to determine cell viability. Panel A: 6 pulse peaks recorded at an average 500,000 ng/mL. Panel B: Interpeak intervals recorded at an average of 16.111 minutes between pulse peaks.

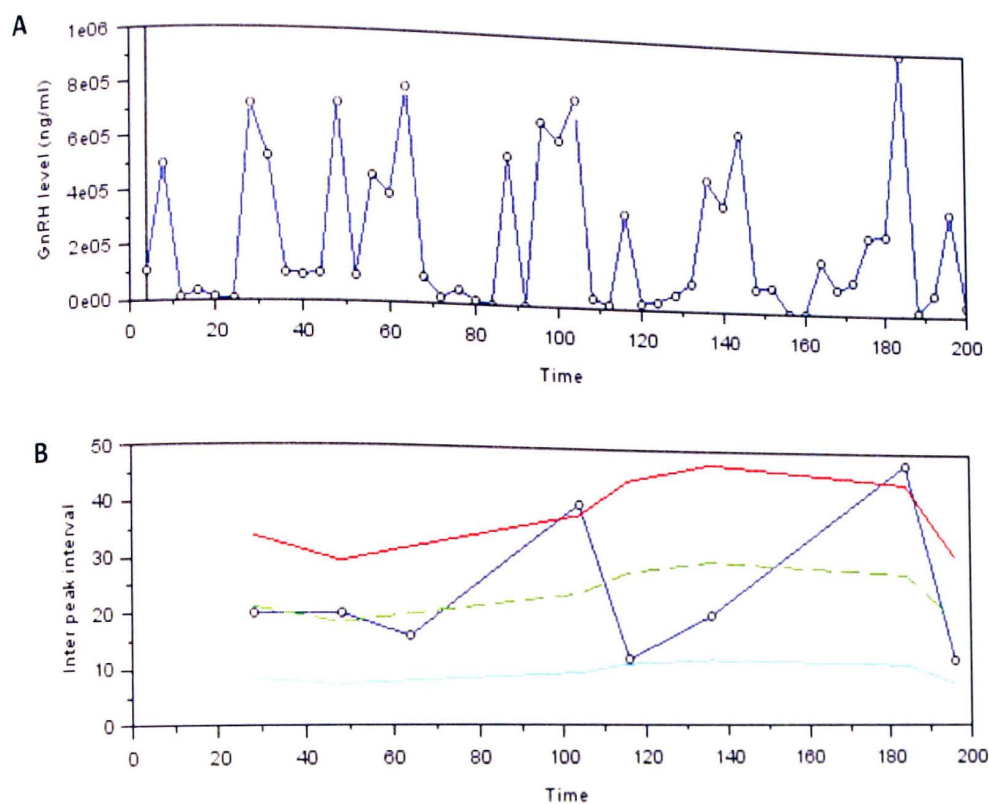


Figure 6: Control culture 6 receiving only Locke's medium for 180 minutes. At 180th minute veratridine was added to determine cell viability. Panel A: 7 pulse peaks recorded at an average 500,000 ng/mL. Panel B: Interpeak intervals recorded at an average of 24.444 minutes between pulse peaks.

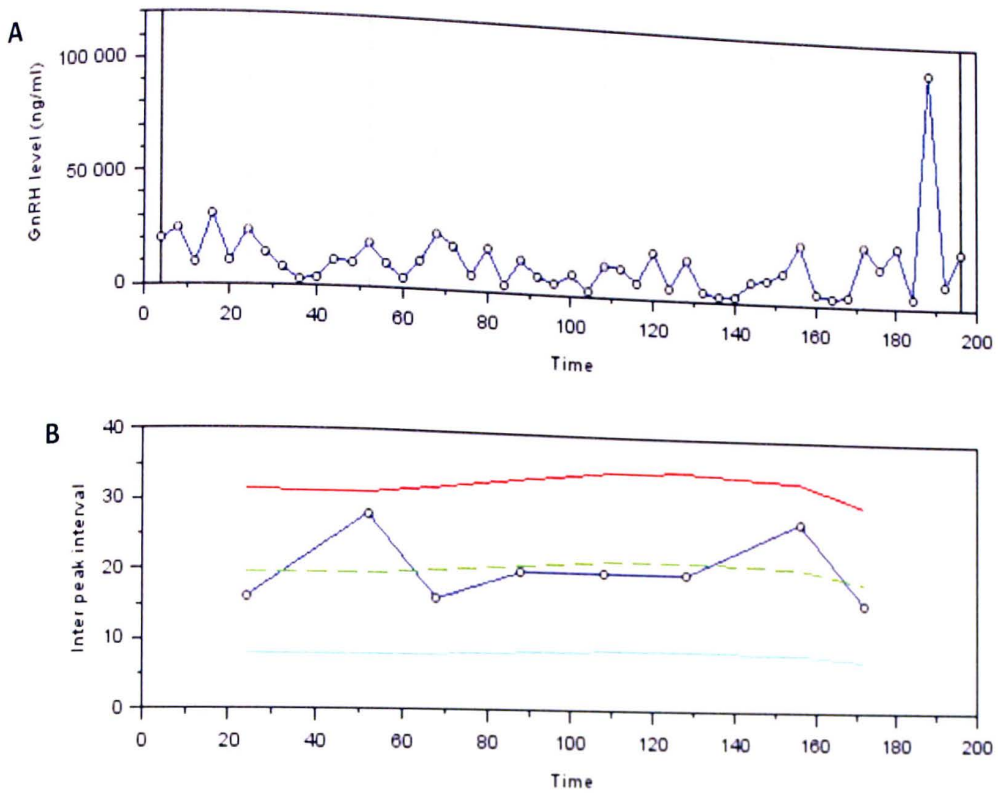


Figure 7: Control culture 7 receiving only Locke's medium for 180 minutes. At 180th minute veratridine was added to determine cell viability. Panel A: 9 pulse peaks recorded at an average 25,000 ng/mL. Panel B: Interpeak intervals recorded at an average of 19.375 minutes between pulse peaks.

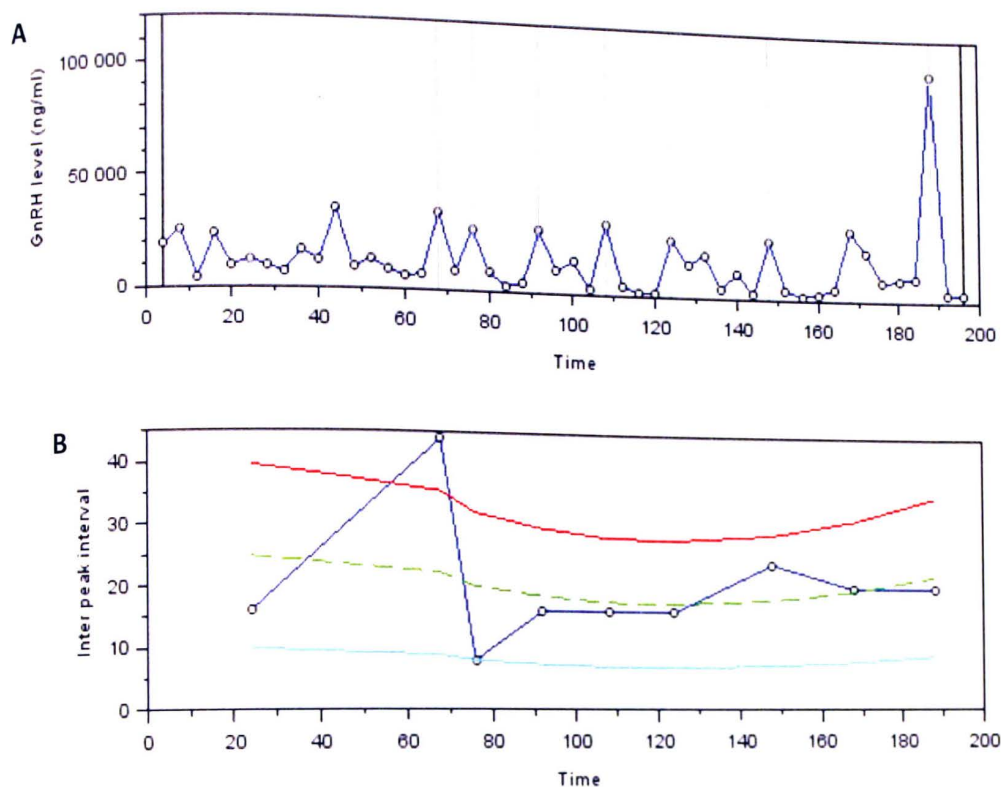


Figure 8: Control culture 8 receiving only Locke's medium for 180 minutes. At 180th minute veratridine was added to determine cell viability. Panel A: 9 pulse peaks recorded at an average 25,000 ng/mL. Panel B: Interpeak intervals recorded at an average of 17.778 minutes between pulse peaks.

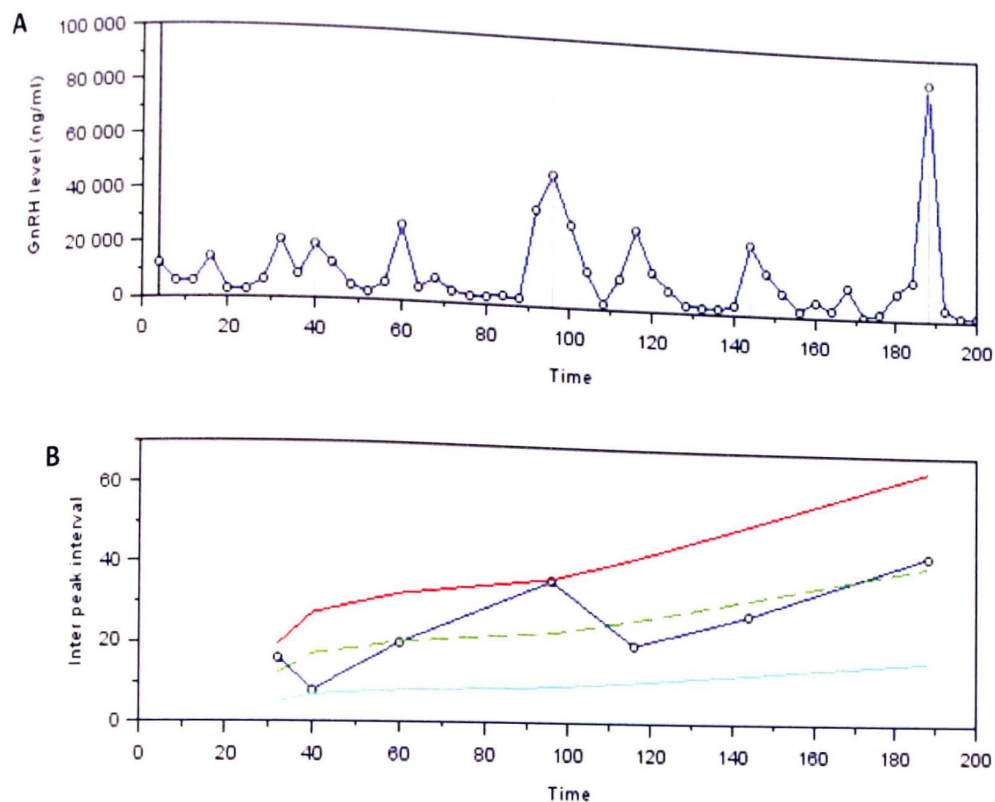


Figure 9: Control culture 9 receiving only Locke's medium for 180 minutes. At 180th minute veratridine was added to determine cell viability. Panel A: 7 pulse peaks recorded at an average 25,000 ng/mL. Panel B: Interpeak intervals recorded at an average of 17.143 minutes between pulse peaks.

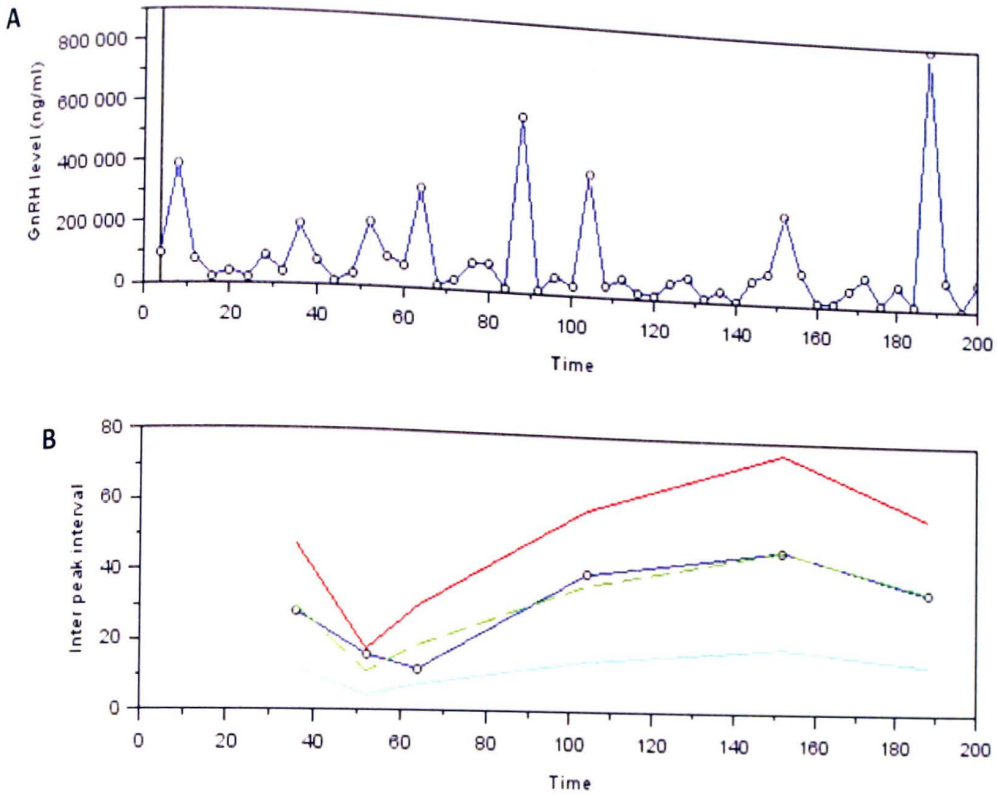


Figure 10: Control culture 10 receiving only Locke's medium for 180 minutes. At 180th minute veratridine was added to determine cell viability. Panel A: 6 pulse peaks recorded at an average 400,000 ng/mL. Panel B: Interpeak intervals recorded at an average of 23.333 minutes between pulse peaks.

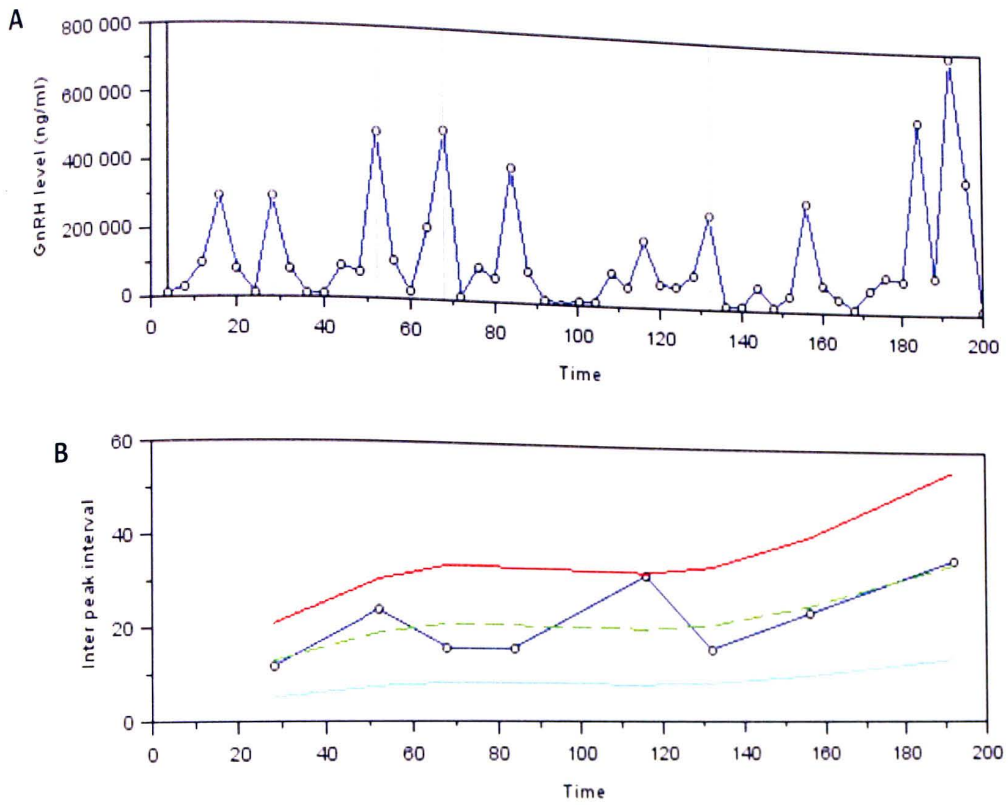


Figure 11: Control culture 11 receiving only Locke's medium for 180 minutes. At 180th minute veratridine was added to determine cell viability. Panel A: 8 pulse peaks recorded at an average 250,000 ng/mL. Panel B: Interpeak intervals recorded at an average of 17.5 minutes between pulse peaks.

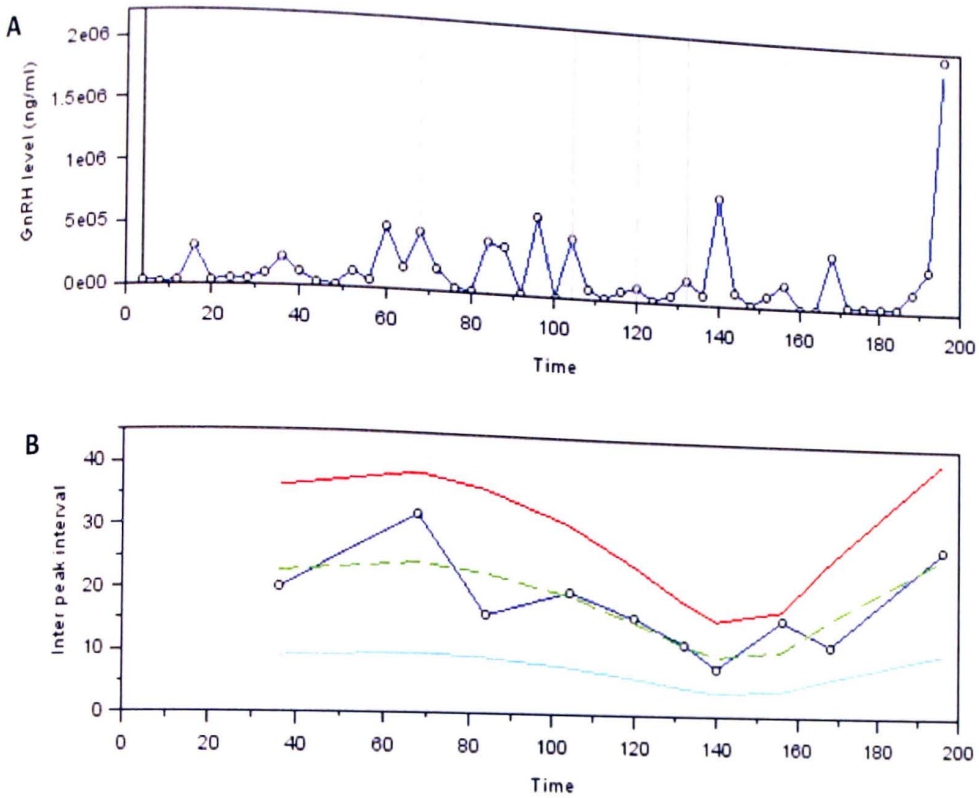


Figure 12: Control culture 12 receiving only Locke's medium for 180 minutes. At 180th minute veratridine was added to determine cell viability. Panel A: 10 pulse peaks recorded at an average 500,000 ng/mL. Panel B: Interpeak intervals recorded at an average of 14 minutes between pulse peaks.

APPENDIX B: Pulse Analysis for Experimental Cells

This appendix contains figures which depict the amount of GnRH secreted by GT1-7 cell cultures that were perfused with 50 μ M ZD7288 dissolved in Locke's medium for 180 minutes. In each figure, Panel A depicts the amount of GnRH secreted during each 4-minute collection period. "True" pulse peaks were determined by the Dynpeak analysis software and are denoted by vertical lines. Panel B is part of the Dynpeak output and shows the true IPI values in blue and corresponds to the duration of time between each pulse peak recorded. The dashed green lines indicate the moving cubic function fitting the values of the IPI series. The lower and upper solid lines indicate the edges of the GnRH tunnel, indicating the normal ranges of pulse peaks expected throughout each series. Unusually high or low pulse peaks are indicated by their occurrence outside of the GnRH tunnel, and indicate the possibility of pulse outliers. Unusually high pulse peaks, outside of the tunnel, could suggest that there were multiple 'true' GnRH secretory events that occurred in a short time frame, and results in one large pulse peak being detected. Pulse peaks occurring below the tunnel, signifies a low probability of a true secretory event. GnRH pulses that fell outside GnRH tunnel were not counted as pulse. Peaks after veratridine exposure were not included, but noted for cell viability.

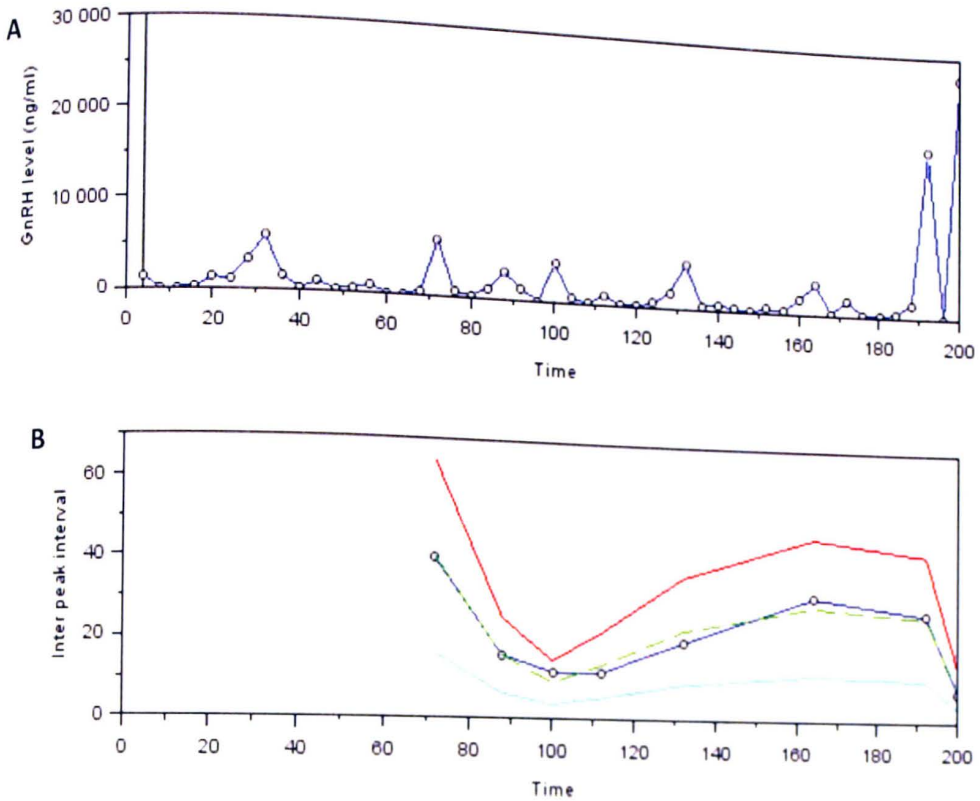


Figure 1: Experimental culture 1 receiving 50 μ M zd7288 dissolved in Locke's medium for 180th minute. At 180th minute veratridine was added to determine cell viability. Panel A: 7 pulse peaks recorded at an average 5,000 ng/mL. Panel B: Interpeak intervals recorded at an average of 21.429 minutes between pulse peaks.

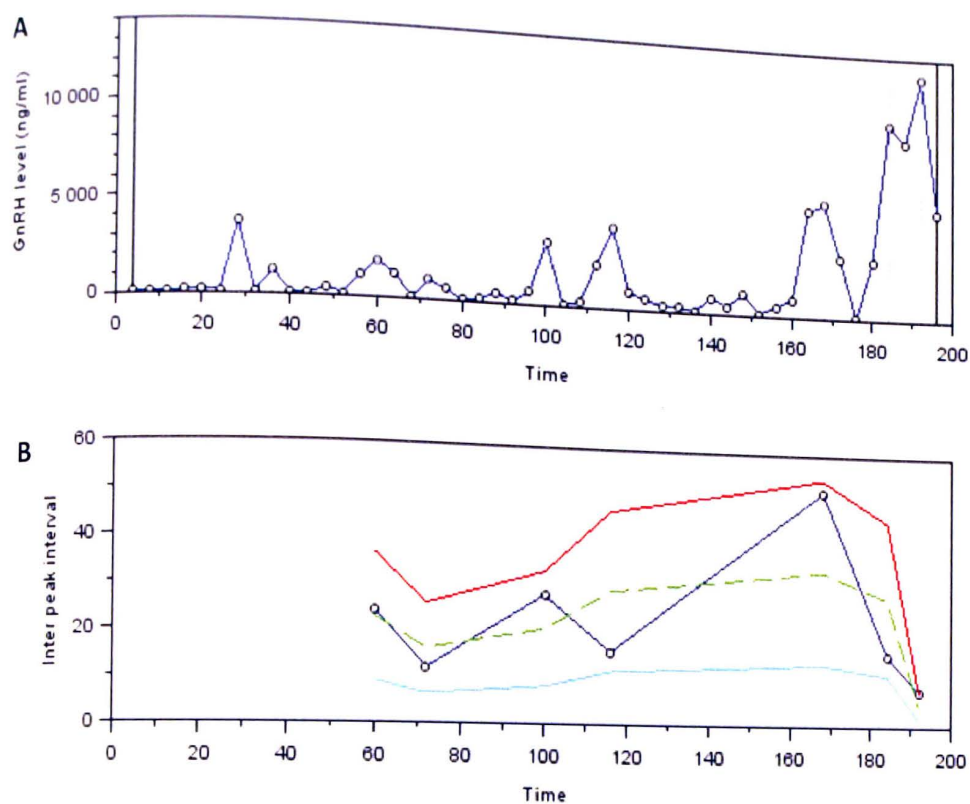


Figure 2: Experimental culture 2 receiving 50 μ M zd7288 dissolved in Locke's medium for 180 minutes. At 180th minute veratridine was added to determine cell viability. Panel A: 6 pulse peaks recorded at an average 4,000 ng/mL. Panel B: Interpeak intervals recorded at an average of 20 minutes between pulse peaks.

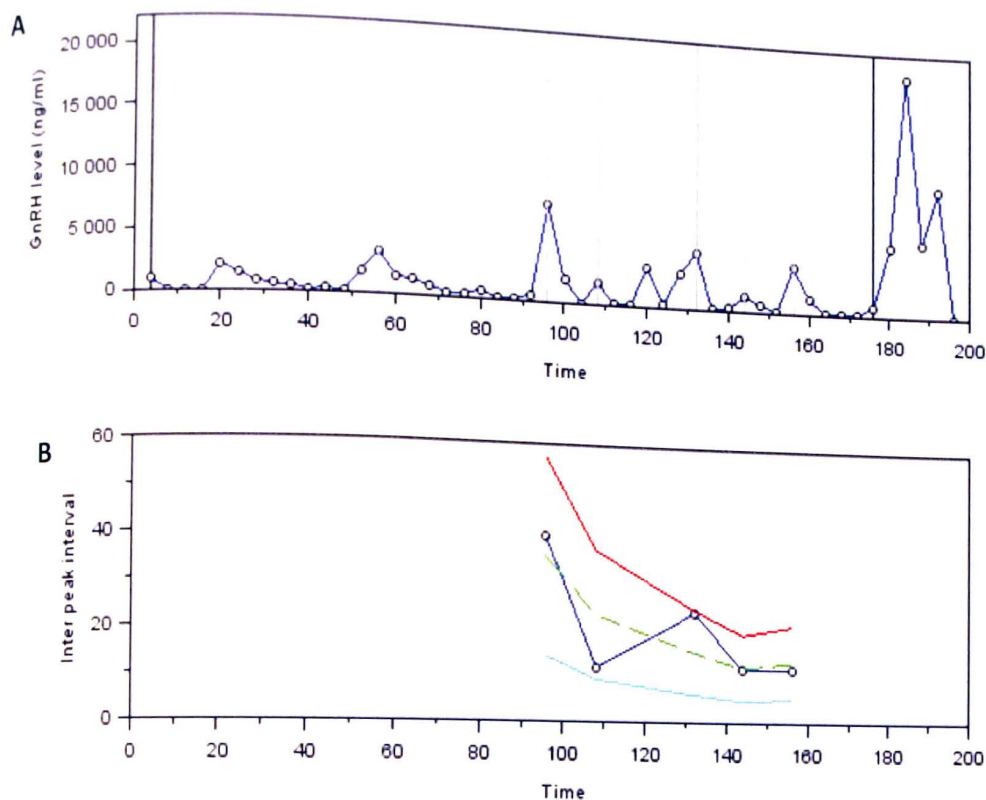


Figure 3: Experimental culture 3 receiving 50 μM zd7288 dissolved in Locke's medium for 180 minutes. At 180th minute veratridine was added to determine cell viability. Panel A: 6 pulse peaks recorded at an average 4,000 ng/mL. Panel B: Interpeak intervals recorded at an average of 20 minutes between pulse peaks.

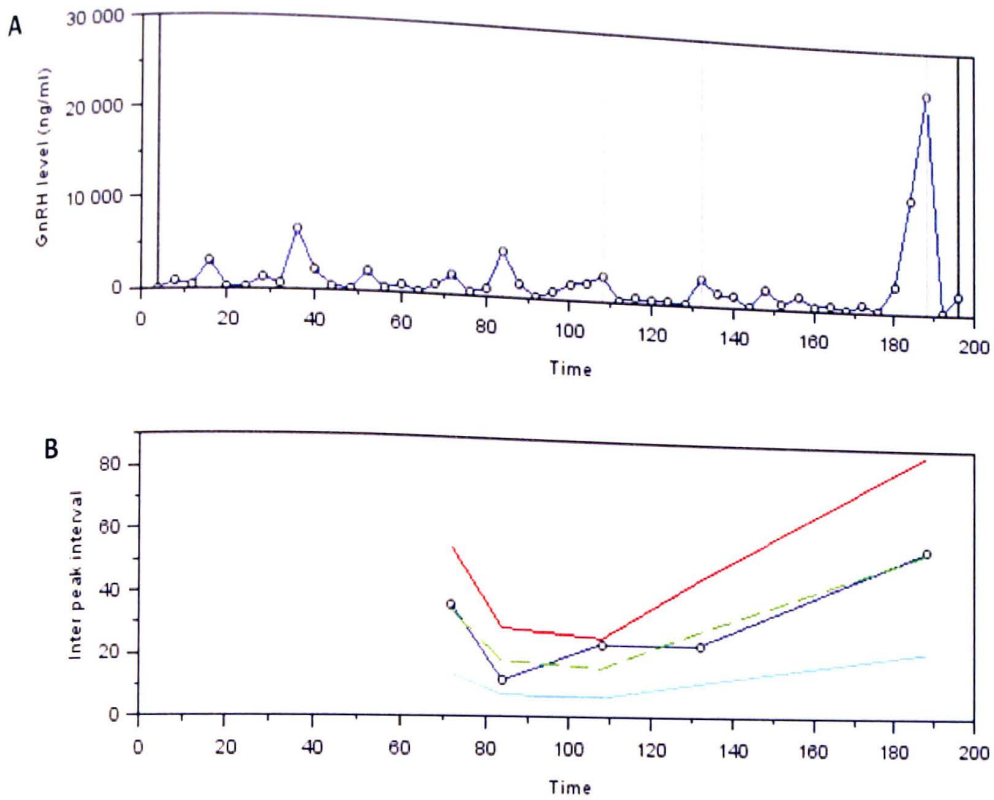


Figure 4: Experimental culture 4 receiving 50 μ M zd7288 dissolved in Locke's medium for 180 minutes. At 180th minute veratridine was added to determine cell viability. Panel A: 5 pulse peaks recorded at an average 5,000 ng/mL. Panel B: Interpeak intervals recorded at an average of 26 minutes between pulse peaks.

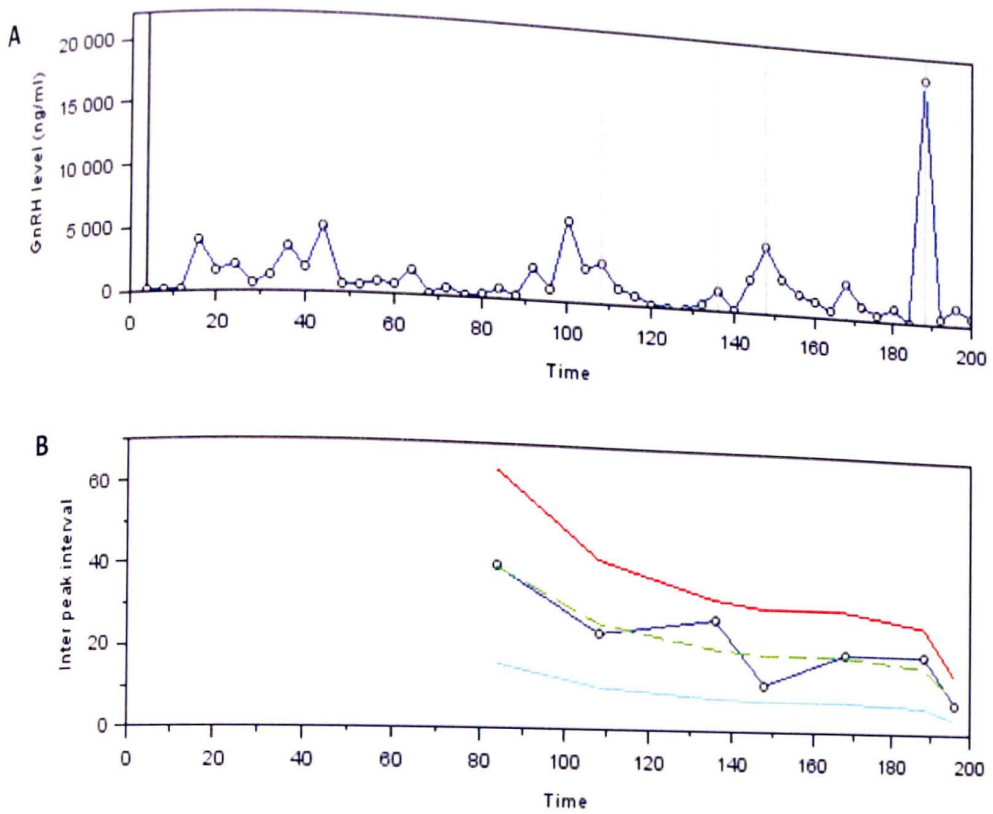


Figure 5: Experimental culture 5 receiving 50 μ M zd7288 dissolved in Locke's medium for 180 minutes. At 180th minute veratridine was added to determine cell viability. Panel A: 6 pulse peaks recorded at an average 4,000 ng/mL. Panel B: Interpeak intervals recorded at an average of 21.429 minutes between pulse peaks.

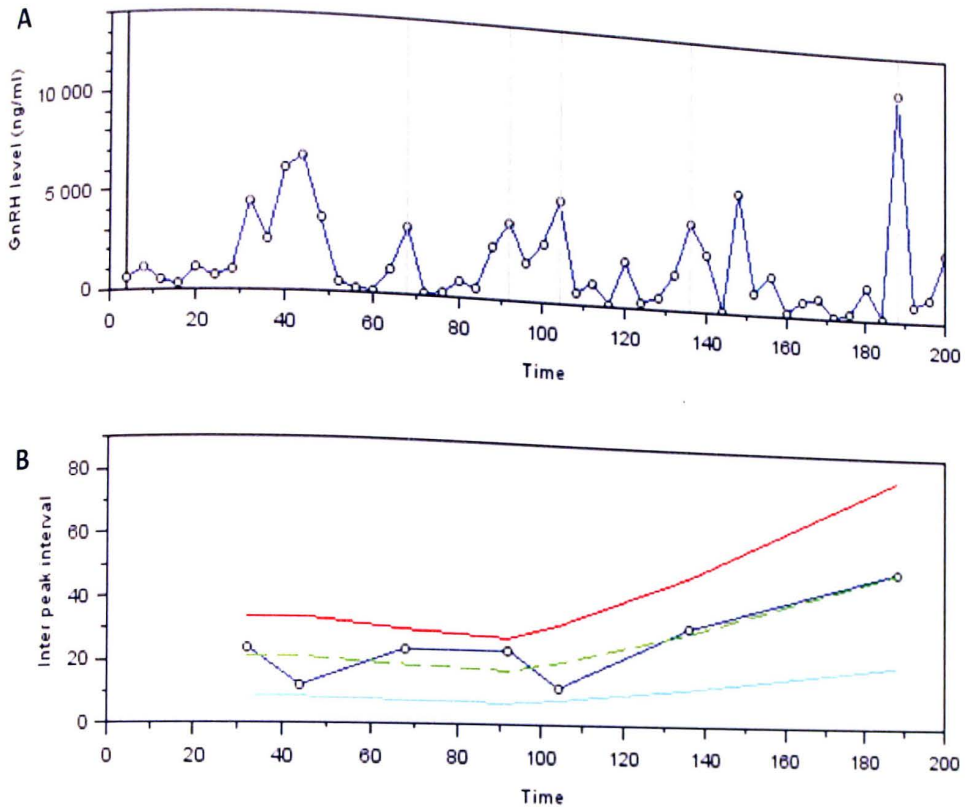


Figure 6: Experimental culture 6 receiving 50 μ M zd7288 dissolved in Locke's medium for 180 minutes. At 180th minute veratridine was added to determine cell viability. Panel A: 7 pulse peaks recorded at an average 5,000 ng/mL. Panel B: Interpeak intervals recorded at an average of 21.429 minutes between pulse peaks.

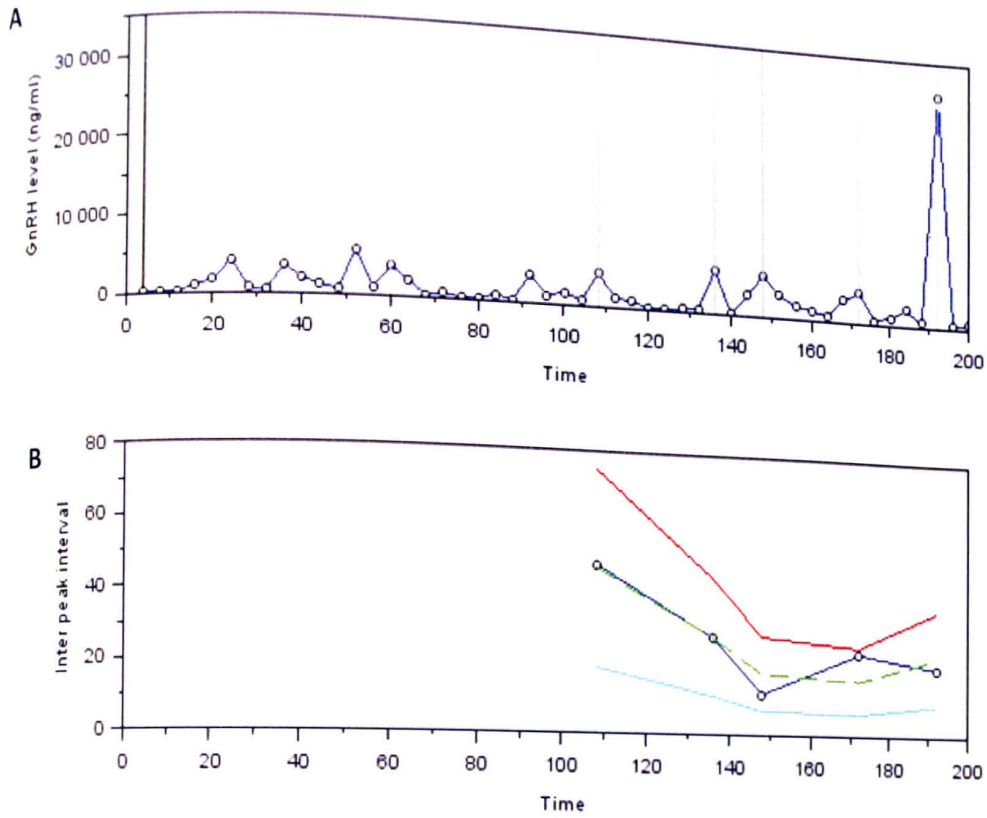


Figure 7: Experimental culture 7 receiving 50 μ M zd7288 dissolved in Locke's medium for 180 minutes. At 180th minute veratridine was added to determine cell viability. Panel A: 5 pulse peaks recorded at an average 5,000 ng/mL. Panel B: Interpeak intervals recorded at an average of 26 minutes between pulse peaks.

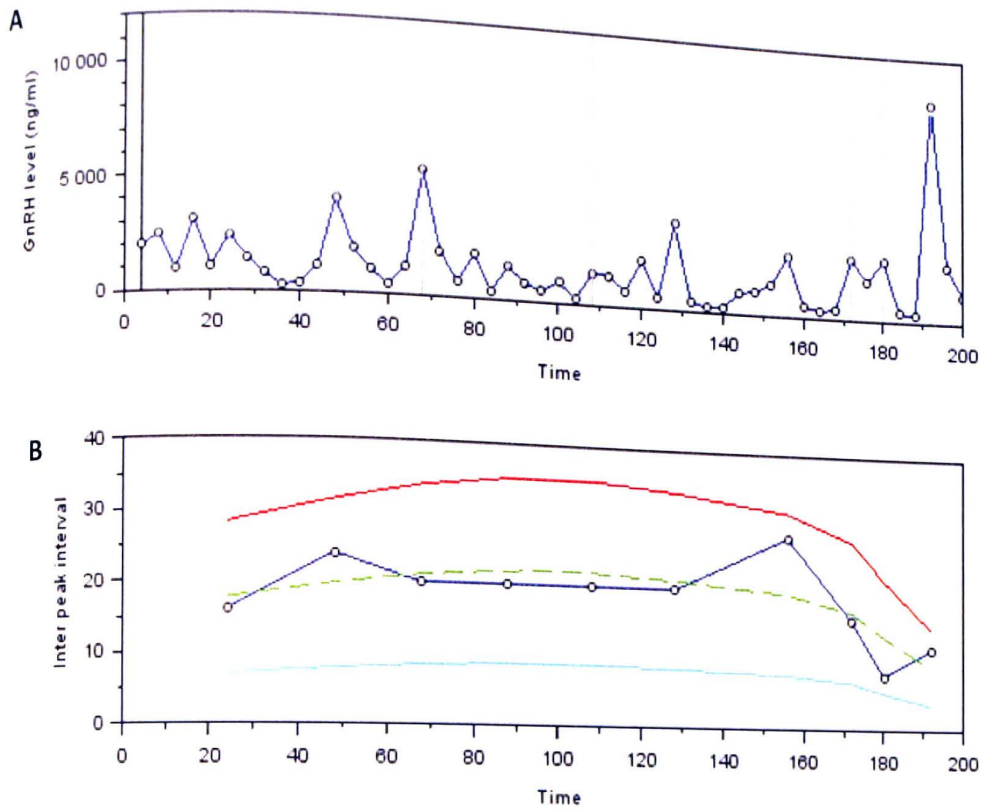


Figure 8: Experimental culture 8 receiving 50 μ M zd7288 dissolved in Locke's medium for 180 minutes. At 180th minute veratridine was added to determine cell viability. Panel A: 9 pulse peaks recorded at an average 3,500 ng/mL. Panel B: Interpeak intervals recorded at an average of 20.628 minutes between pulse peaks.

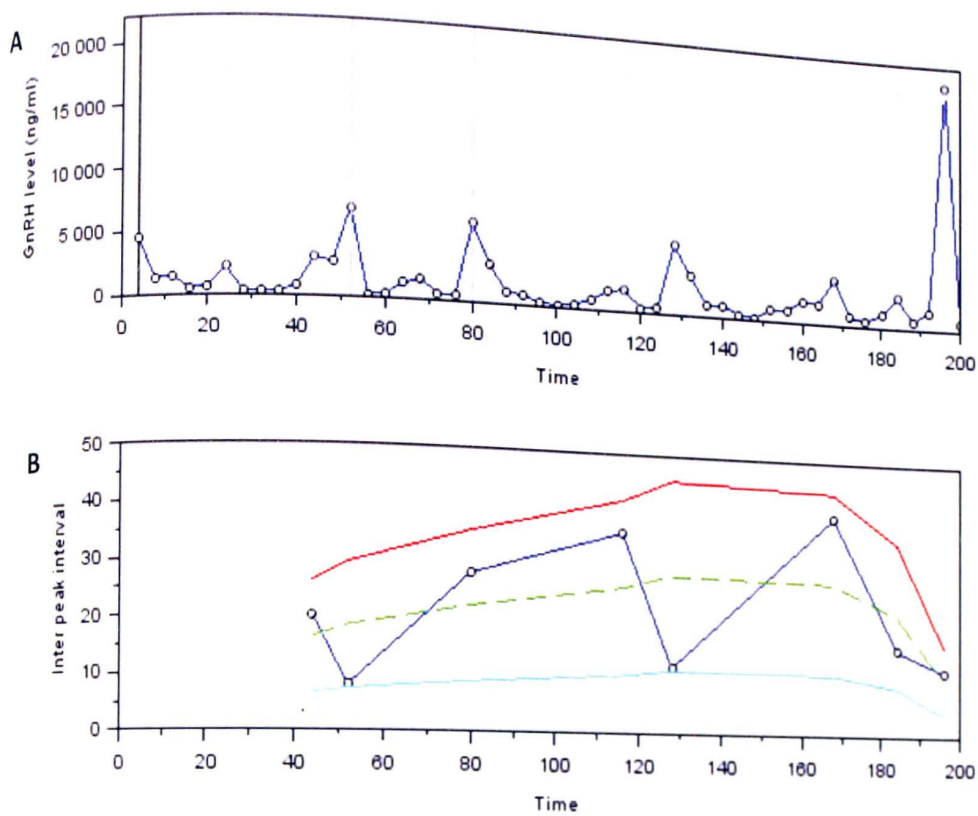


Figure 9: Experimental culture 9 receiving 50 μ M zd7288 dissolved in Locke's medium for 180 minutes. At 180th minute veratridine was added to determine cell viability. Panel A: 7 pulse peaks recorded at an average 5,000 ng/mL. Panel B: Interpeak intervals recorded at an average of 21.429 minutes between pulse peaks.

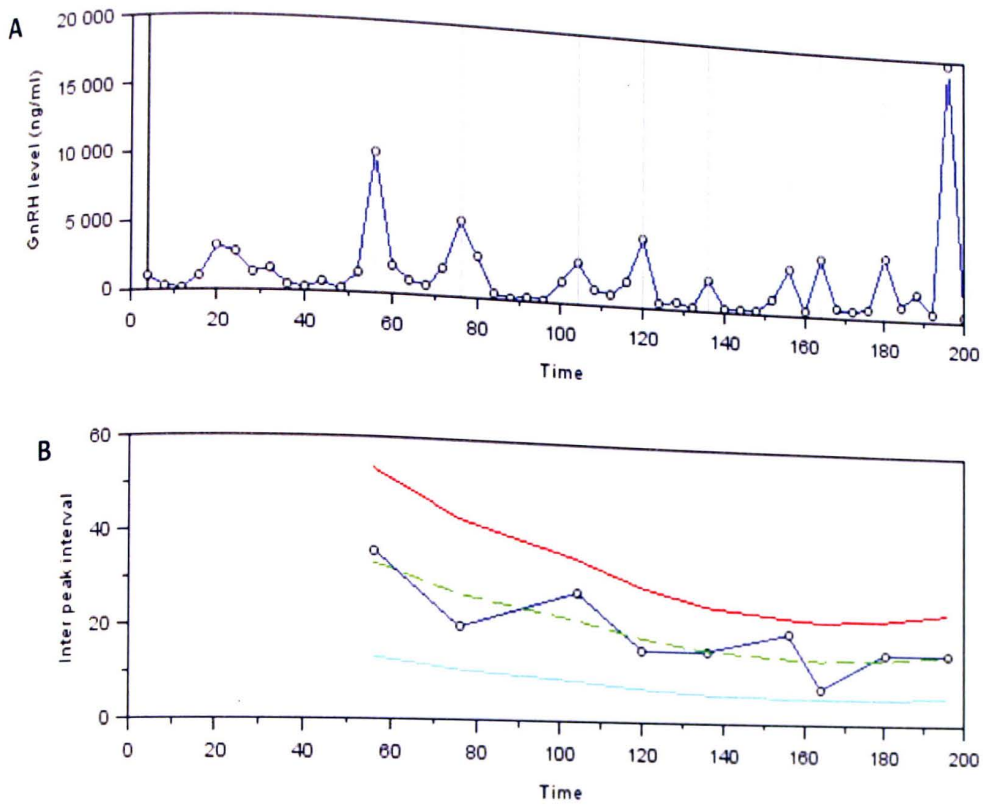


Figure 10: Experimental culture 10 receiving 50 μ M zd7288 dissolved in Locke's medium for 180 minutes. At 180th minute veratridine was added to determine cell viability. Panel A: 8 pulse peaks recorded at an average 5,000 ng/mL. Panel B: Interpeak intervals recorded at an average of 18.75 minutes between pulse peaks.

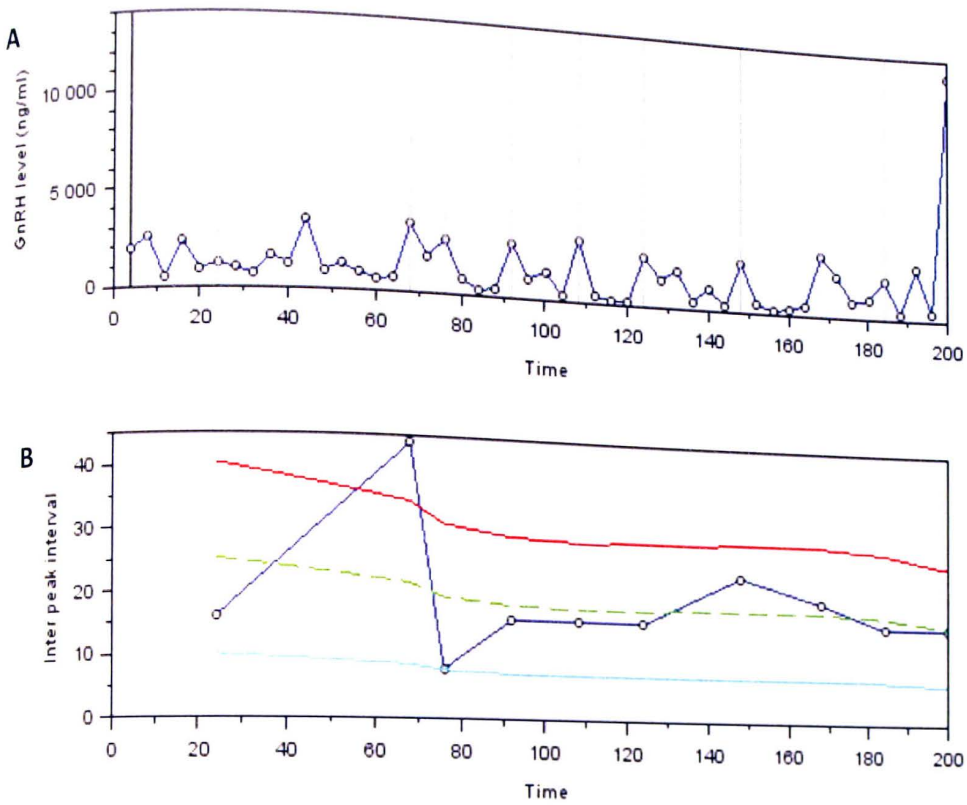


Figure 11: Experimental culture 11 receiving 50 μM zd7288 dissolved in Locke's medium for 180 minutes. At 180th minute veratridine was added to determine cell viability. Panel A: 9 pulse peaks recorded at an average 4,000 ng/mL. Panel B: Interpeak intervals recorded at an average of 22.778 minutes between pulse peaks.

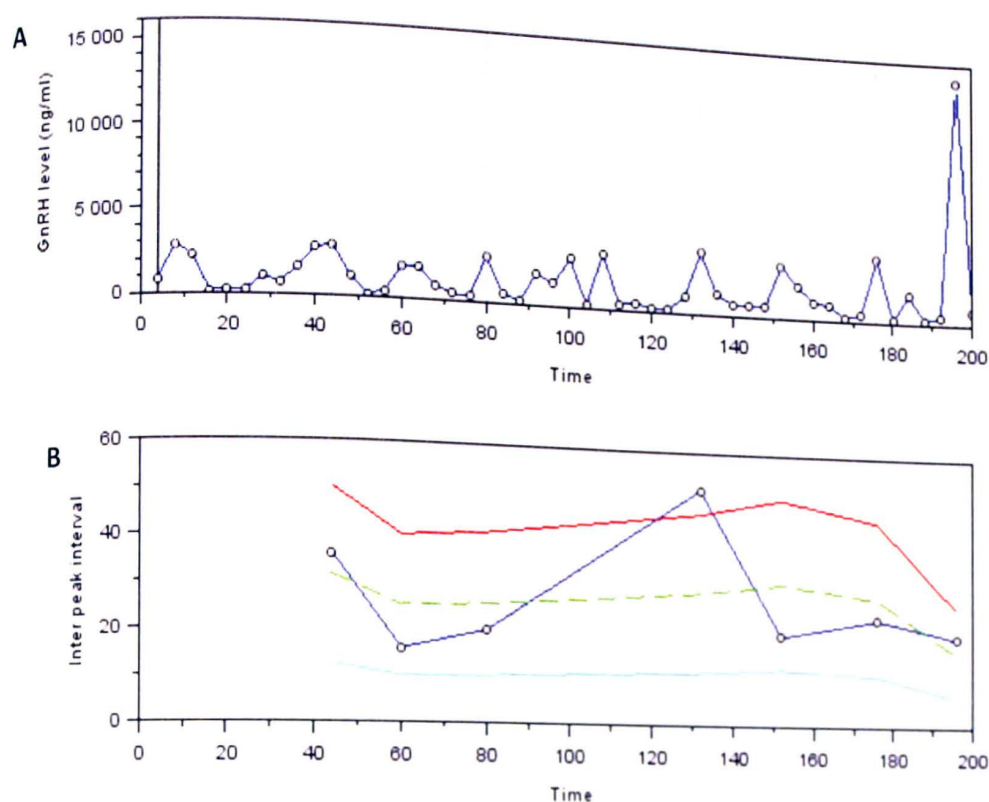


Figure 12: Experimental culture 12 receiving 50 μ M zd7288 dissolved in Locke's medium for 180 minutes. At 180th minute veratridine was added to determine cell viability. Panel A: 7 pulse peaks recorded at an average 4,000 ng/mL. Panel B: Interpeak intervals recorded at an average of 27.143 minutes between pulse peaks.

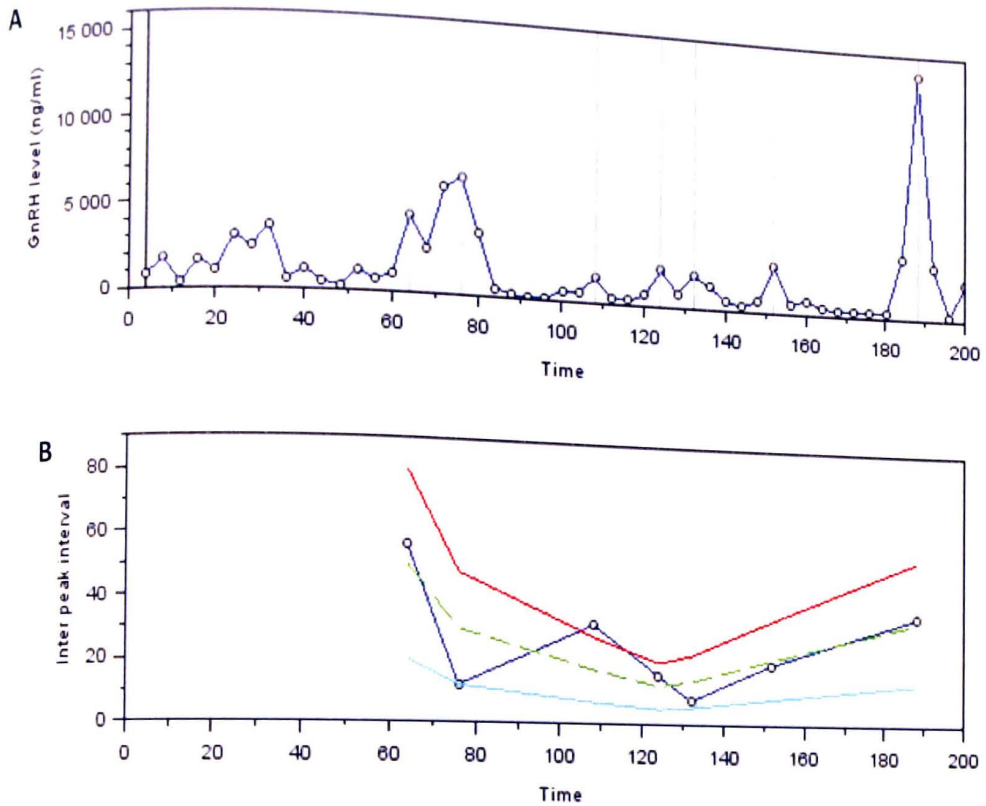


Figure 13: Experimental culture 13 receiving 50 μ M zd7288 dissolved in Locke's medium for 180 minutes. At 180th minute veratridine was added to determine cell viability. Panel A: 7 pulse peaks recorded at an average 3,500 ng/mL. Panel B: Interpeak intervals recorded at an average of 25.714 minutes between pulse peaks.

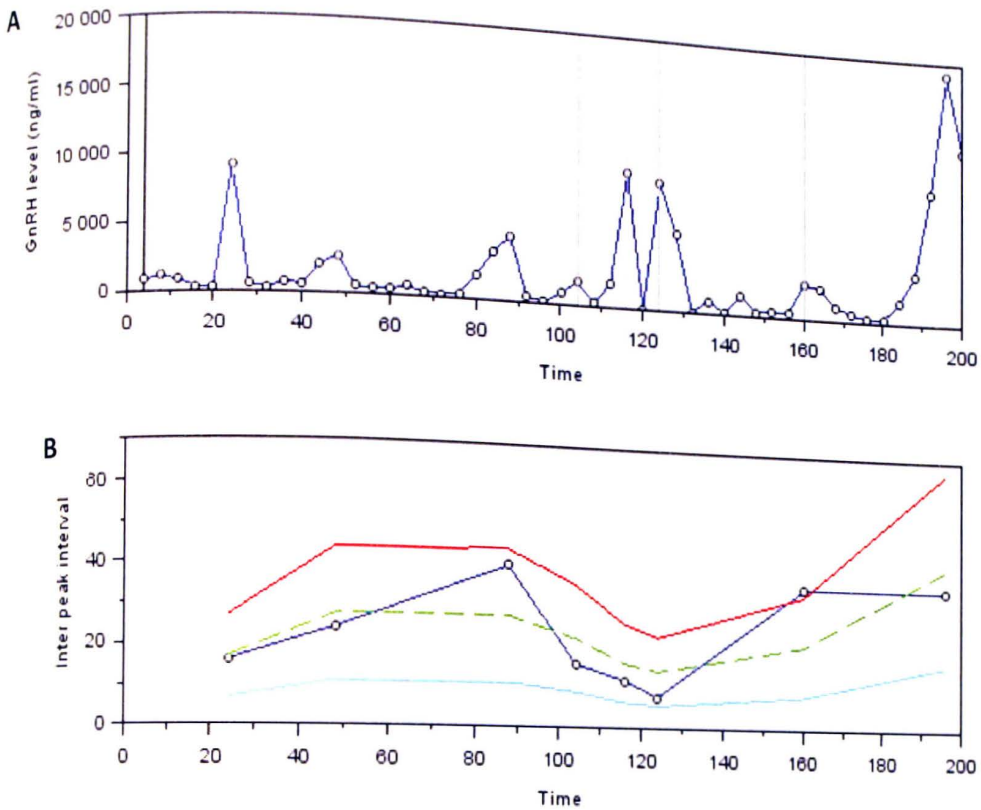


Figure 14: Experimental culture 14 receiving 50 μ M zd7288 dissolved in Locke's medium for 180 minutes. At 180th minute veratridine was added to determine cell viability. Panel A: 8 pulse peaks recorded at an average 8,000 ng/mL. Panel B: Interpeak intervals recorded at an average of 25.625 minutes between pulse peaks.

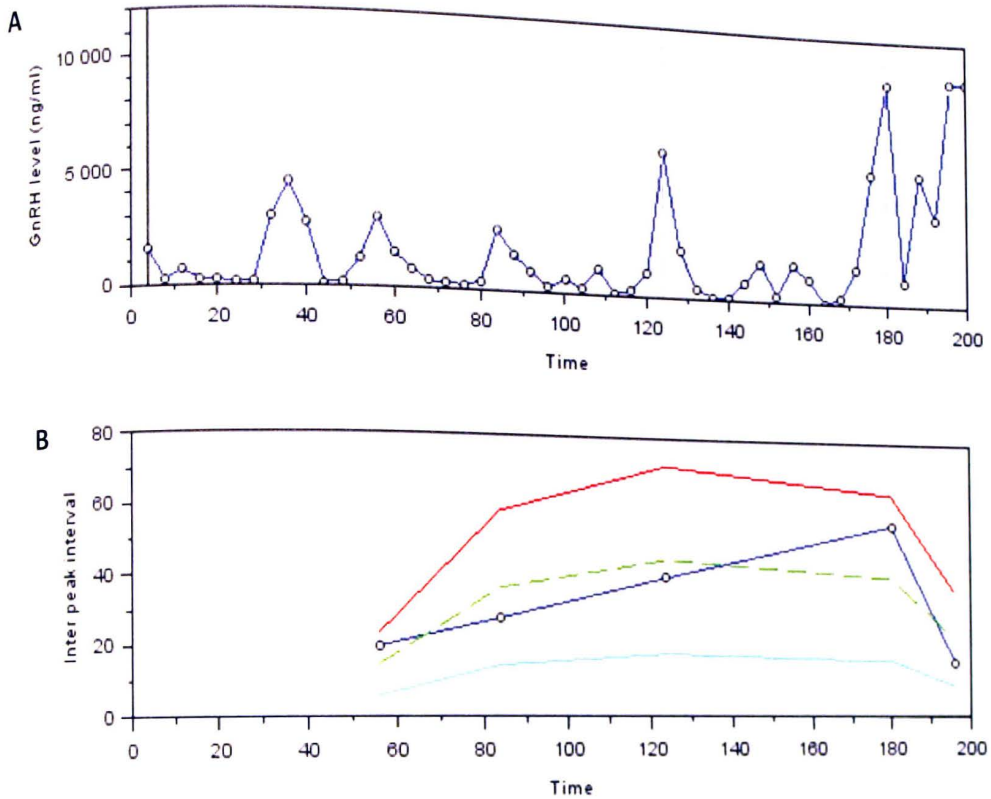


Figure 15: Experimental culture 15 receiving 50 μ M zd7288 dissolved in Locke's medium for 180 minutes. At 180th minute veratridine was added to determine cell viability. Panel A: 4 pulse peaks recorded at an average 4,000 ng/mL. Panel B: Interpeak intervals recorded at an average of 32 minutes between pulse peaks.

APPENDIX C: Pulse Analysis for Sequential Cells

This appendix contains figures which depict the amount of GnRH secreted by GT1-7 cell cultures that were perfused with Locke's medium for 120 minutes, then perfused with 50 μ M ZD7288 for an additional 120 minutes. In each figure, Panel A depicts the amount of GnRH secreted during each 4-minute collection period. "True" pulse peaks were determined by the Dynpeak analysis software and are denoted by vertical lines. Panel B is part of the Dynpeak output and shows the true IPI values in blue and corresponds to the duration of time between each pulse peak recorded. The dashed green lines indicate the moving cubic function fitting the values of the IPI series. The lower and upper solid lines indicate the edges of the GnRH tunnel, indicating the normal ranges of pulse peaks expected throughout each series. Unusually high or low pulse peaks are indicated by their occurrence outside of the GnRH tunnel, and indicate the possibility of pulse outliers. Unusually high pulse peaks, outside of the tunnel, could suggest that there were multiple 'true' GnRH secretory events that occurred in a short time frame, and results in one large pulse peak being detected. Pulse peaks occurring below the tunnel, signifies a low probability of a true secretory event. GnRH pulses that fell outside GnRH tunnel were not counted as pulse. Peaks after veratridine exposure were not included, but noted for cell viability. Some figures veratridine peaks were low or undetected, these were noted by at least a 5% increase in pulse peak within the raw data. Some veratridine peaks and pulse peaks were undetected by dynpeak software because it adjusts pulse peak determination based on the highest detectable value. ZD7288 is shown to markedly reduce veratridine effect when occurring sequentially after ZD7288 exposure.

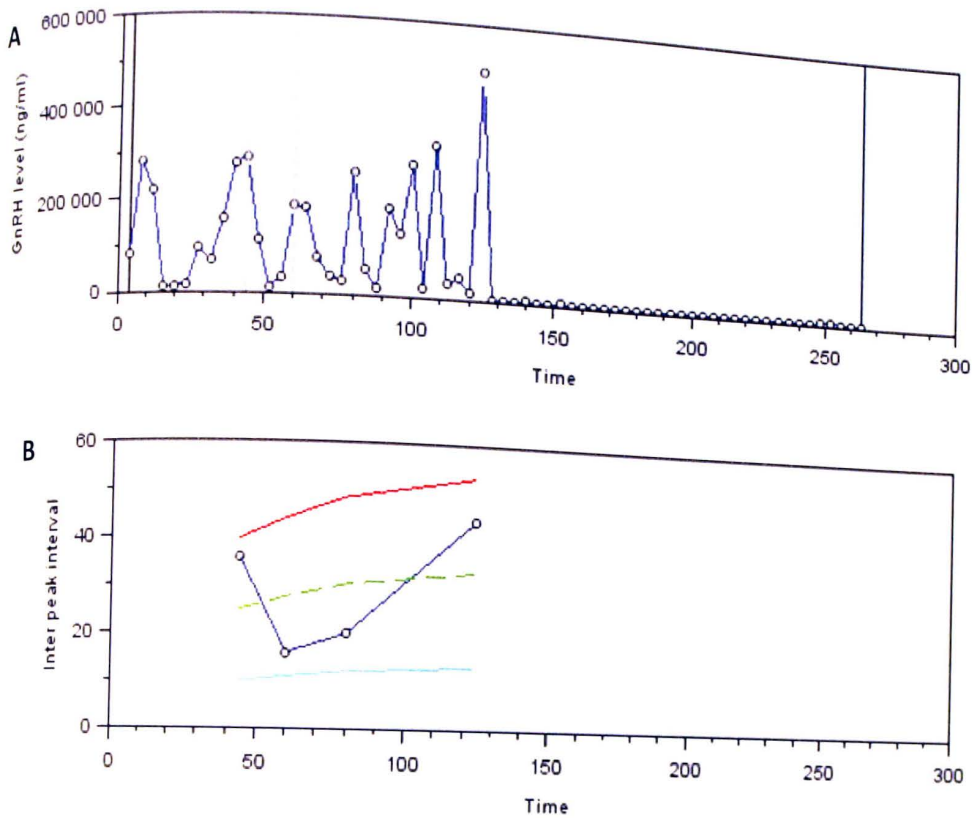


Figure 1: Sequential culture 1 receiving Locke's medium for 120 minutes, then treated with 50 μ M zd7288 dissolved in Locke's medium for 120 minutes. At 240th minute veratridine was added to determine cell viability. Panel A: 4 pulse peaks recorded at an average 300,000 ng/mL. Panel B: Interpeak intervals recorded at an average of 25 minutes between pulse peaks. Panel A and Panel B: Pulse peaks were undetectable after addition of zd7288.

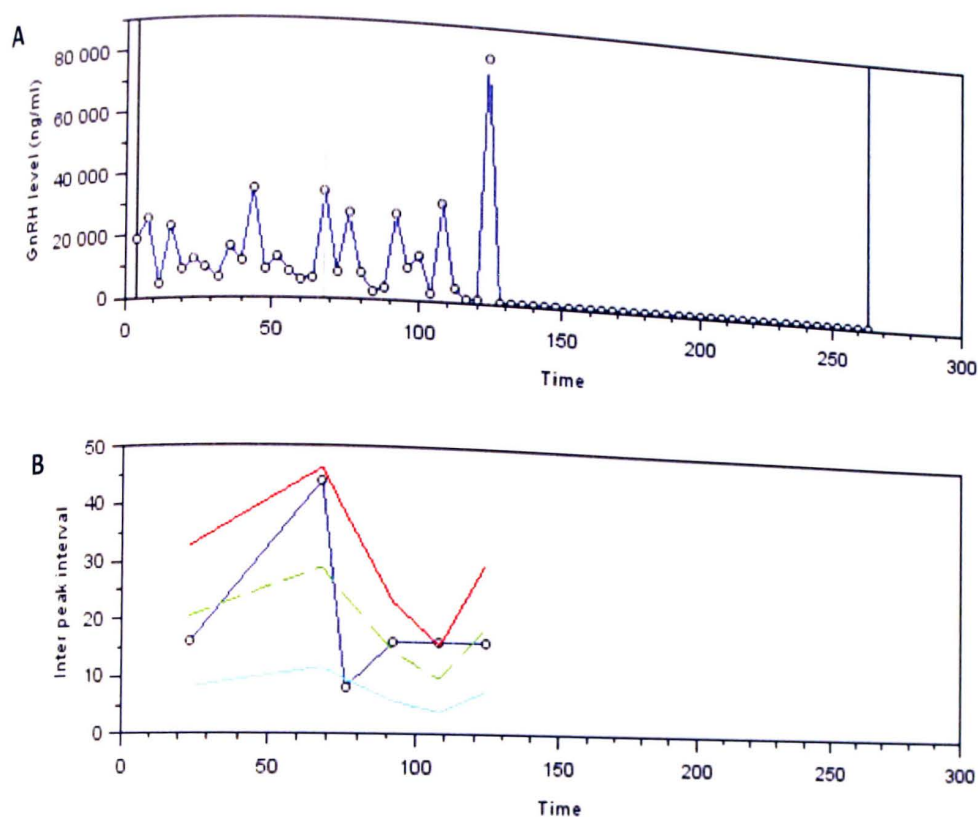


Figure 2: Sequential culture 2 receiving Locke's medium for 120 minutes, then treaded with 50 μ M zd7288 dissolved in Locke's medium for 120 minutes. At 240th minute veratridine was added to determine cell viability. Panel A: 6 pulse peaks recorded at an average 30,000 ng/mL. Panel B: Interpeak intervals recorded at an average of 24.1667 minutes between pulse peaks. Panel A and Panel B: Pulse peaks were undetectable after addition of zd7288.

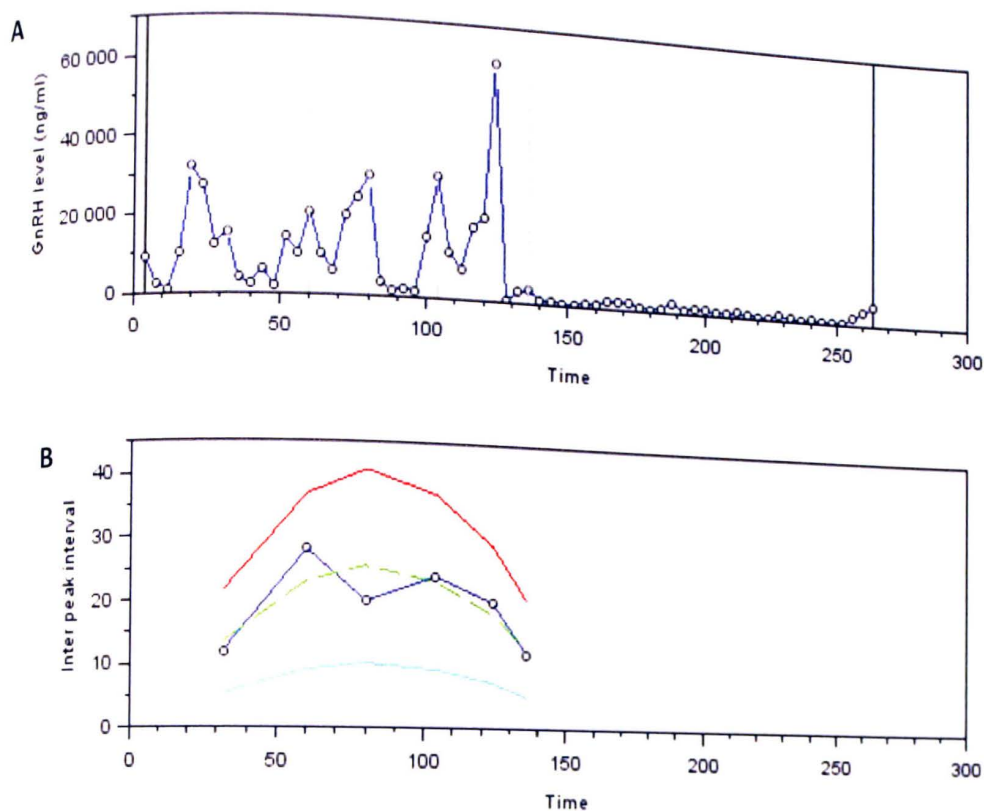


Figure 3: Sequential culture 3 receiving Locke's medium for 120 minutes, then treated with 50 μ M zd7288 dissolved in Locke's medium for 120 minutes. At 240th minute veratridine was added to determine cell viability. Panel A: 6 pulse peaks recorded at an average 30,000 ng/mL. Panel B: Interpeak intervals recorded at an average of 19.1667 minutes between pulse peaks. Panel A and Panel B: Pulse peaks were undetectable after addition of zd7288.

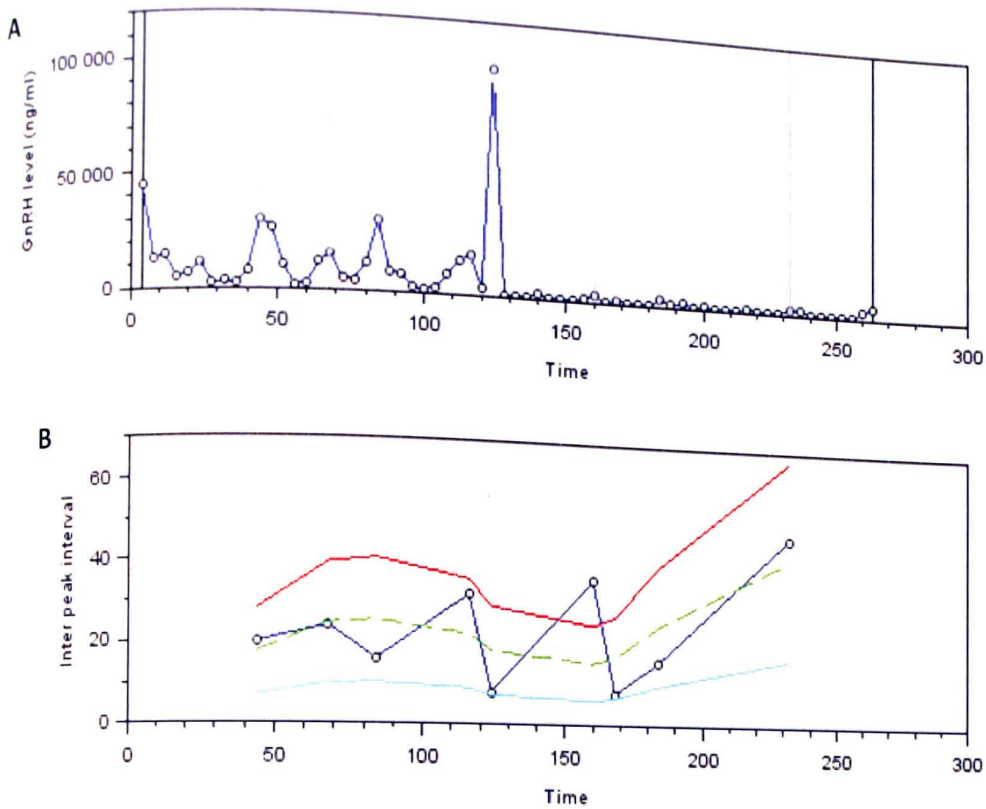


Figure 4: Sequential culture 4 receiving Locke's medium for 120 minutes, then treaded with 50 μ M zd7288 dissolved in Locke's medium for 120 minutes. At 240th minute veratridine was added to determine cell viability. Panel A: 5 pulse peaks recorded at an average 30,000 ng/mL. Panel B: Interpeak intervals recorded at an average of 17 minutes between pulse peaks. Panel A: 4 pulse peaks were detected at an average of 3,000 ng/mL, with an interpeak interval of 27.5 minutes after addition of zd7288 (Panel B).

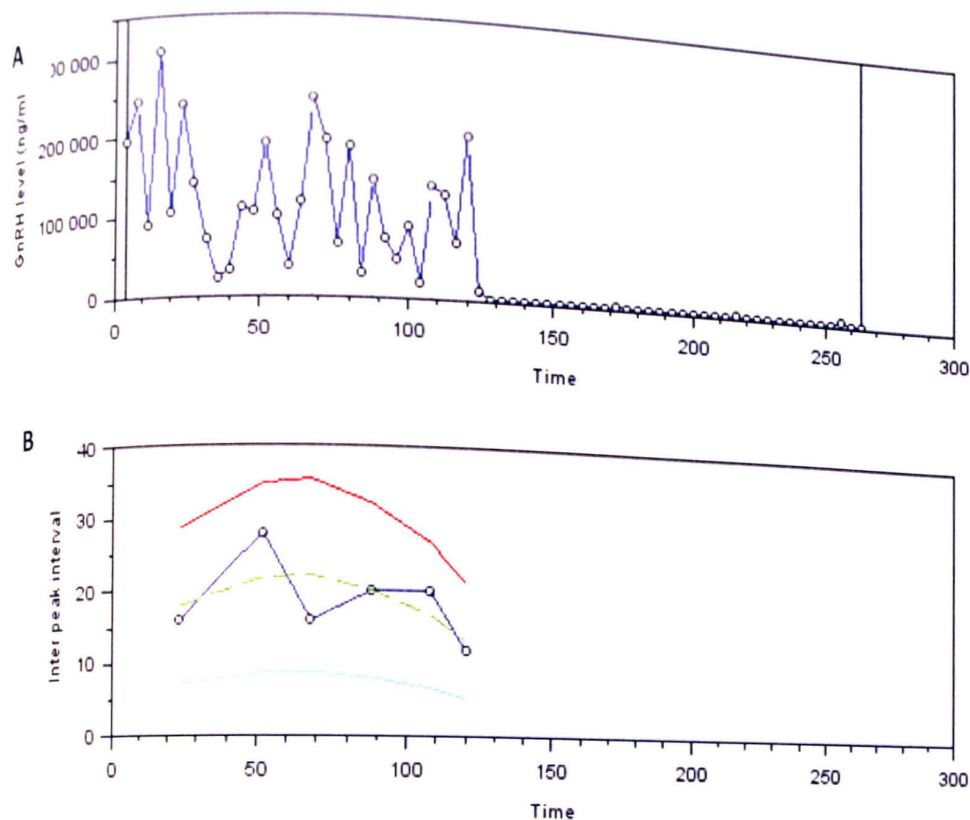


Figure 5: Sequential culture 5 receiving Locke's medium for 120 minutes, then treated with 50 μ M zd7288 dissolved in Locke's medium for 120 minutes. At 240th minute veratridine was added to determine cell viability. Panel A: 6 pulse peaks recorded at an average 250,000 ng/mL. Panel B: Interpeak intervals recorded at an average of 18.333 minutes between pulse peaks. Panel A and Panel B: Pulse peaks were undetectable after addition of zd7288.

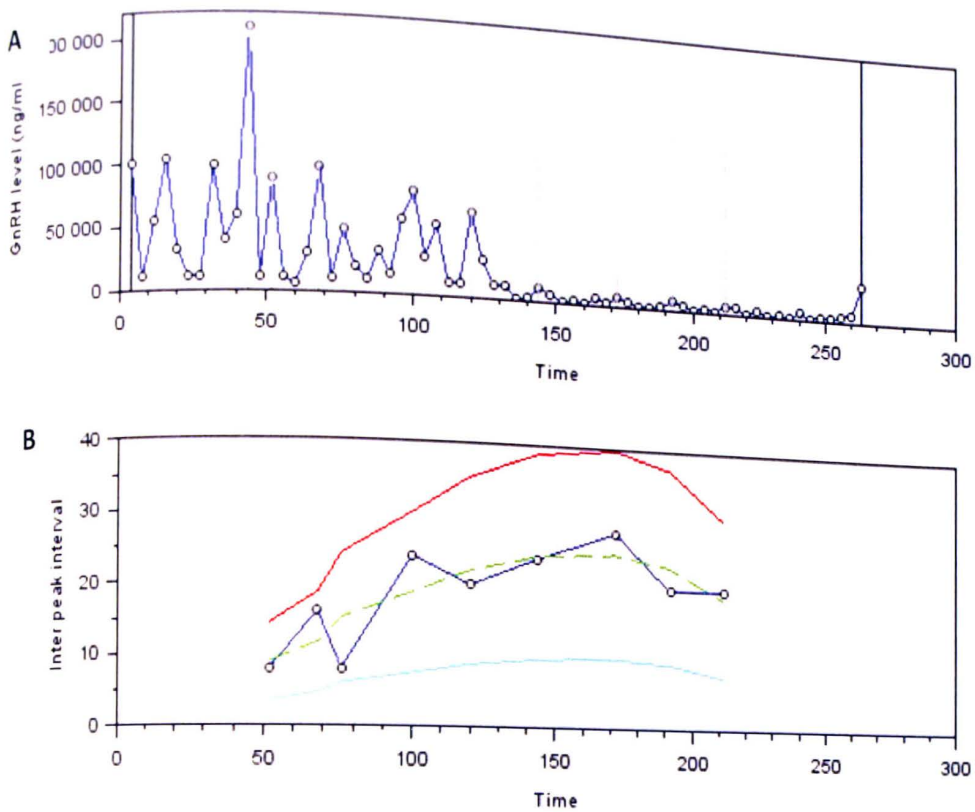


Figure 6: Sequential culture 6 receiving Locke's medium for 120 minutes, then treaded with 50 μ M zd7288 dissolved in Locke's medium for 120 minutes. At 240th minute veratridine was added to determine cell viability. Panel A: 5 pulse peaks recorded at an average 300,000 ng/mL. Panel B: Interpeak intervals recorded at an average of 14 minutes between pulse peaks. Panel A: 4 pulse peaks were detected at an average of 3,000 ng/mL, with an interpeak interval of 23.75 minutes after addition of zd7288 (Panel B).

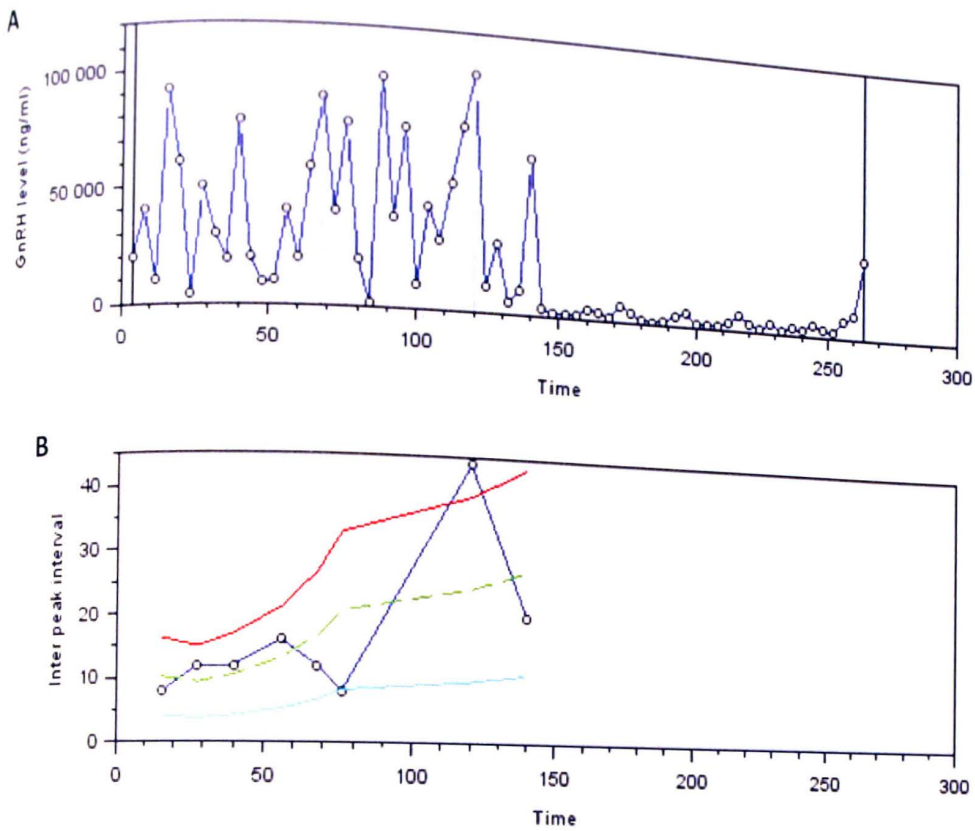


Figure 7: Sequential culture 7 receiving Locke's medium for 120 minutes, then treaded with 50 μ M zd7288 dissolved in Locke's medium for 120 minutes. At 240th minute veratridine was added to determine cell viability. Panel A: 8 pulse peaks recorded at an average 80,000 ng/mL. Panel B: Interpeak intervals recorded at an average of 15 minutes between pulse peaks. Panel A and Panel B: Pulse peaks were undetectable after addition of zd7288.

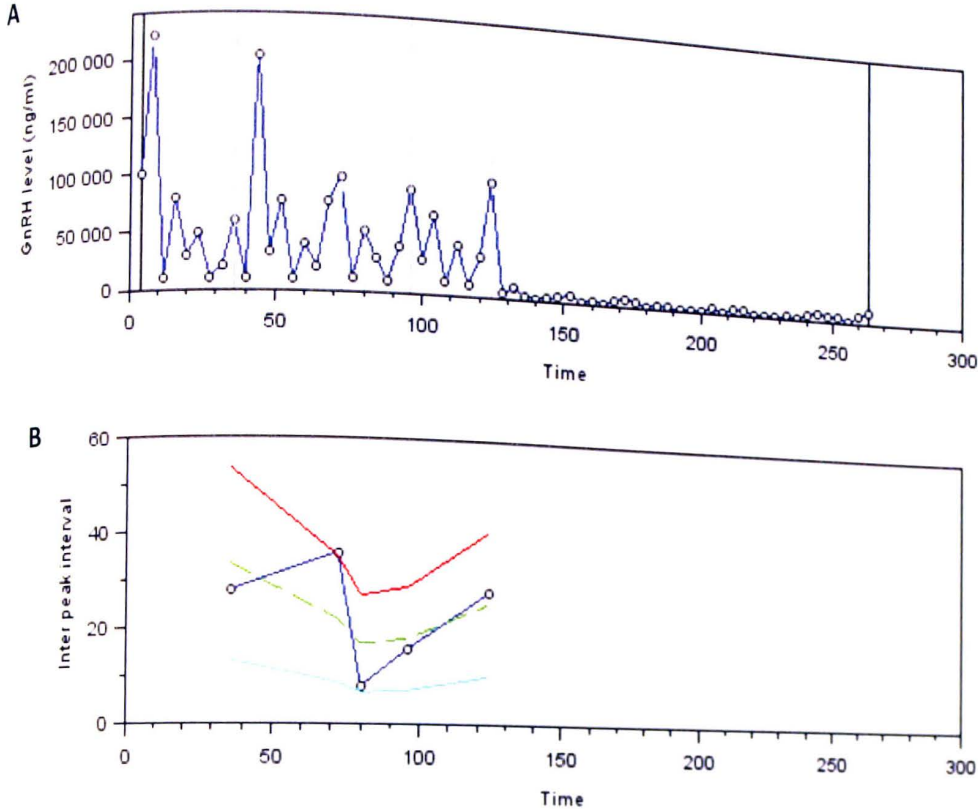


Figure 8: Sequential culture 8 receiving Locke's medium for 120 minutes, then treaded with 50 μ M zd7288 dissolved in Locke's medium for 120 minutes. At 240th minute veratridine was added to determine cell viability. Panel A: 5 pulse peaks recorded at an average 120,000 ng/mL. Panel B: Interpeak intervals recorded at an average of 24 minutes between pulse peaks. Panel A and Panel B: Pulse peaks were undetectable after addition of zd7288.

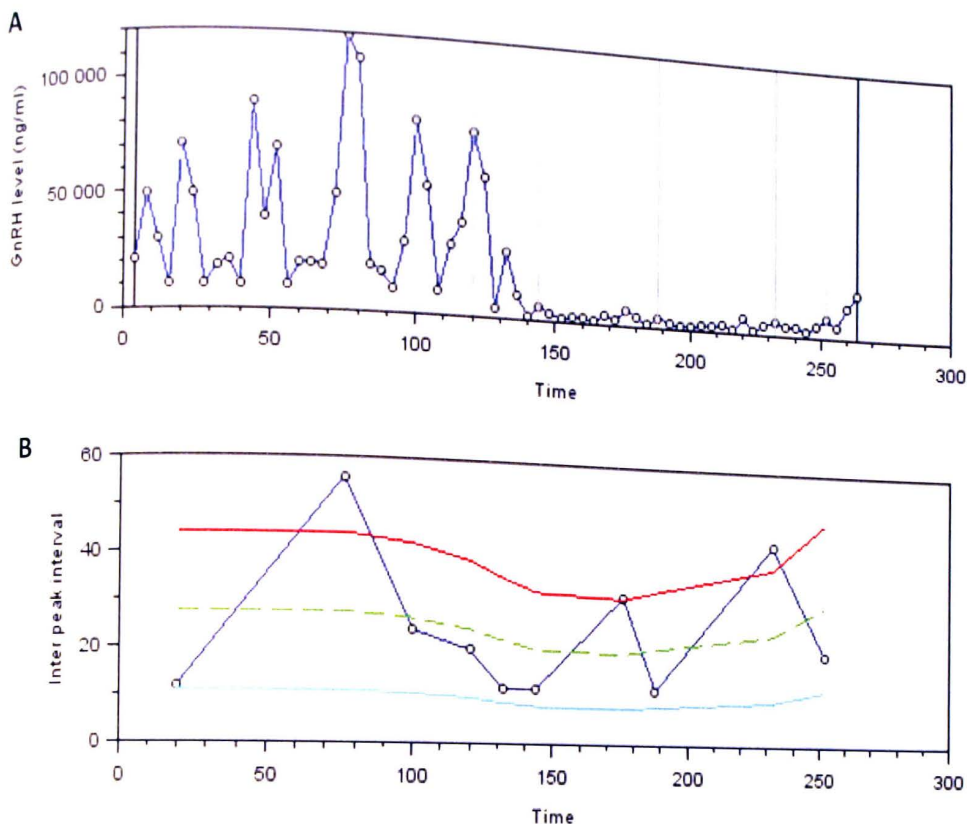


Figure 9: Sequential culture 9 receiving Locke's medium for 120 minutes, then treaded with 50 μ M zd7288 dissolved in Locke's medium for 120 minutes. At 240th minute veratridine was added to determine cell viability. Panel A: 6 pulse peaks recorded at an average 80,000 ng/mL. Panel B: Interpeak intervals recorded at an average of 20 minutes between pulse peaks. Panel A: 3 pulse peaks were detected at an average of 3,000 ng/mL, with an interpeak interval of 27.5 minutes after addition of zd7288 (Panel B).

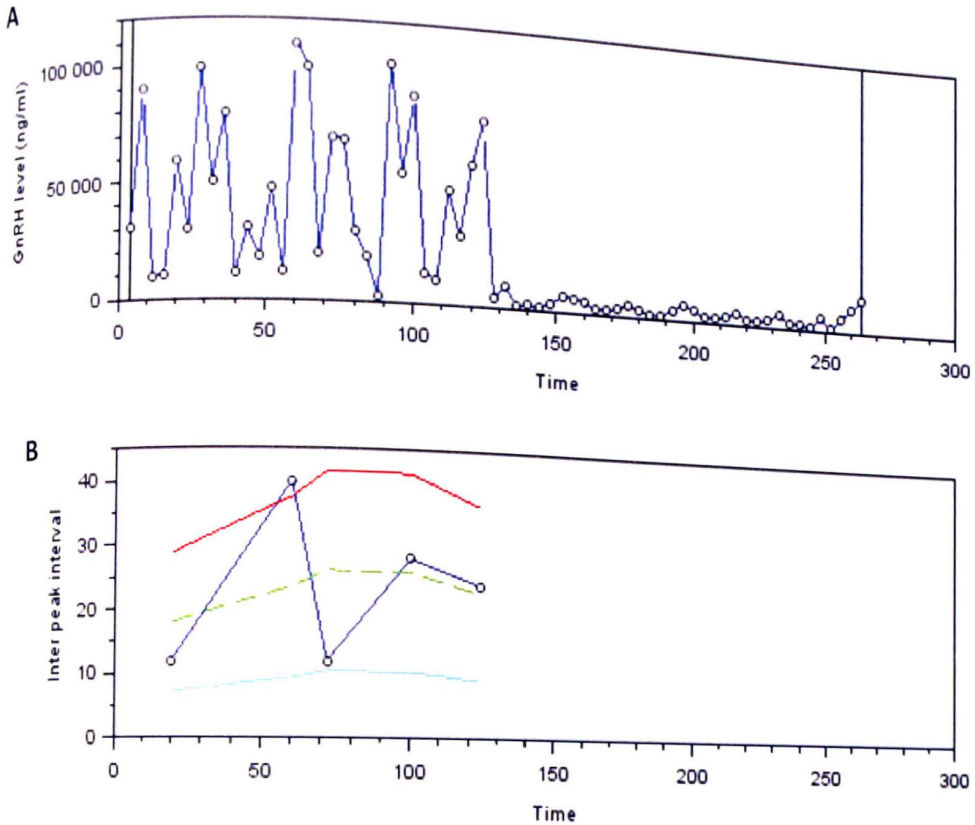


Figure 10: Sequential culture 10 receiving Locke's medium for 120 minutes, then treated with 50 μ M zd7288 dissolved in Locke's medium for 120 minutes. At 240th minute veratridine was added to determine cell viability. Panel A: 4 pulse peaks recorded at an average 100,000 ng/mL. Panel B: Interpeak intervals recorded at an average of 21 minutes between pulse peaks. Panel A and B: Pulse peaks were undetectable after addition of zd7288.

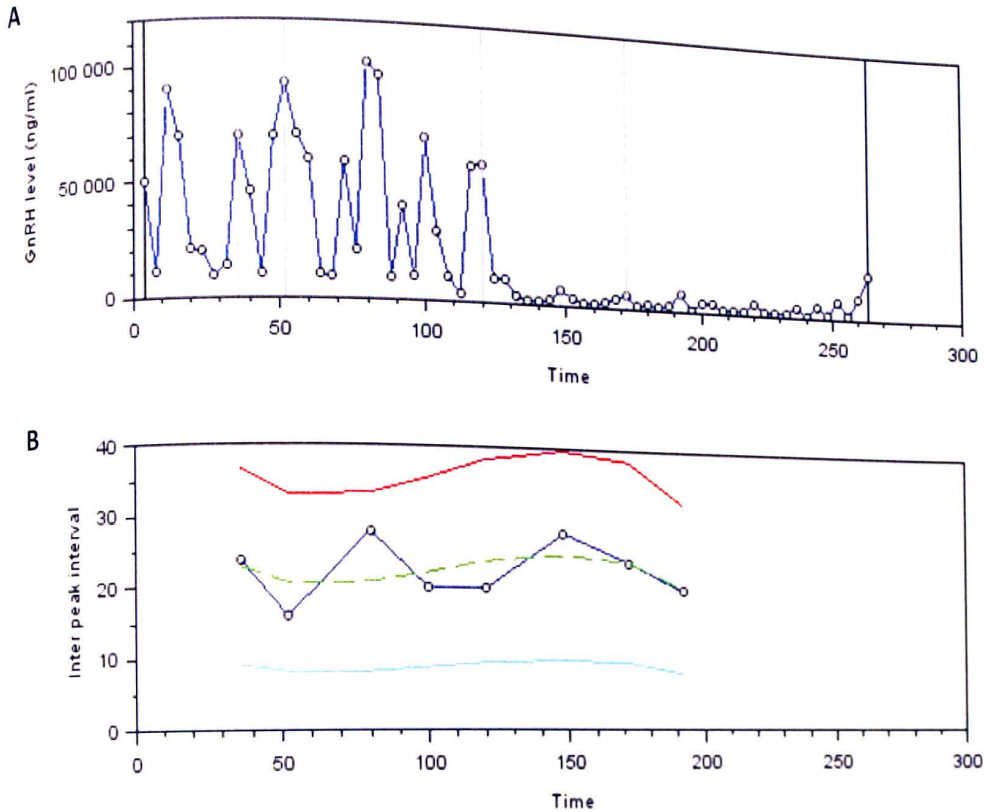


Figure 11: Sequential culture 11 receiving Locke's medium for 120 minutes, then treated with 50 μ M zd7288 dissolved in Locke's medium for 120 minutes. At 240th minute veratridine was added to determine cell viability. Panel A: 5 pulse peaks recorded at an average 80,000 ng/mL. Panel B: Interpeak intervals recorded at an average of 22.5 minutes between pulse peaks. Panel A: 3 pulse peaks were detected at an average of 3,000 ng/mL, with an interpeak interval of 28 minutes after addition of zd7288 (Panel B).

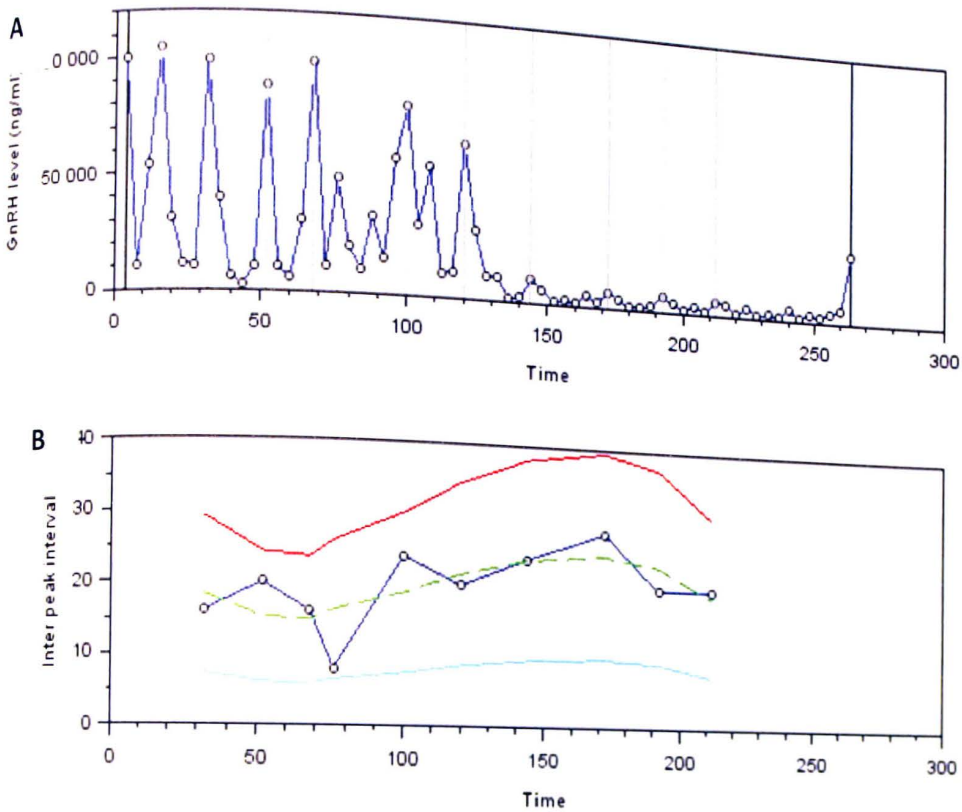


Figure 12: Sequential culture 12 receiving Locke's medium for 120 minutes, then treated with 50 μ M zd7288 dissolved in Locke's medium for 120 minutes. At 240th minute veratridine was added to determine cell viability. Panel A: 7 pulse peaks recorded at an average 80,000 ng/mL. Panel B: Interpeak intervals recorded at an average of 17.14 minutes between pulse peaks. Panel A: 3 pulse peaks were detected at an average of 3,000 ng/mL, with an interpeak interval of 21.667 minutes after addition of zd7288 (Panel B).

APPENDIX D: Data Summary

This appendix contains a table which depicts the summary of data collected from each experimental run. In the first segment, the quantified number of true pulse peaks detected by the dynpeak software is recorded for comparison. These are then summarized by their overall means and standard error reports. The second segment is the Mean interpeak intervals, recorded in minutes, which were observed within each experimental procedure. The final segment of summarized data is the Average GnRH pulse amplitudes, which were observed within each experimental procedure, excluding veratridine pulse peaks which were only noted for cell viability at the end of each procedure. This data summary provides a compiled section for data analysis and comparison between different treatments, a concise form of information to allow the peer review process to analyze and compare the data collected, for future continuations of the study between HCN channels and GnRH secretion.

Table 1:	Number of GnRH Pulse Peaks	Number of GnRH Pulse Peaks	Number of GnRH Pulse Peaks	Number of GnRH Pulse Peaks
Experiment	control	experimental	sequential control	sequential experimental
1	10	7	5	0
2	7	6	6	0
3	8	6	6	1
4	9	5	6	4
5	11	6	7	0
6	9	7	5	4
7	9	5	9	0
8	10	9	6	0
9	8	7	7	4
10	7	8	6	0
11	9	7	6	3
12	10	7	7	4
13		7		
14		8		
15		4		
mean	8.916667	6.6	6.333333	1.666667
stdev	0.35799	1.298351	1.073087	1.922751
sqrt	3.464102	3.872983	3.464102	3.464102
Sterror	0.103343	0.335233	0.309773	0.55505
	Mean IPI (minutes)	Mean IPI (minutes)	Mean IPI (minutes)	Mean IPI (minutes)
Experiment	control	experimental	sequential control	sequential experimental
1	16.667	21.428	25	undetectable
2	25.833	20	24.167	undetectable
3	17.143	20	19.167	undetectable
4	13.75	26	17	27.5
5	16.111	21.428	18.333	Undetectable
6	24.444	21.428	14	23.75
7	19.375	26	15	Undetectable
8	17.778	20.625	24	Undetectable
9	17.143	21.428	20	27.5
10	23.333	18.75	21	Undetectable
11	17.5	22.778	22.5	20

12	14	27.142	17.143	27.5
13		25.714		
14		25.625		
15		32		
	Average Pulse Amplitude (ng/mL)	Average Pulse Amplitude (ng/mL)	Average Pulse Amplitude (ng/mL)	Average Pulse Amplitude (ng/mL)
Experiment	control	experimental	sequential control	sequential experimental
1	50,000	5,000	300,000	undetectable
2	250,000	4,000	30,000	undetectable
3	250,000	4,000	30,000	undetectable
4	80,000	5,000	30,000	<3,000
5	500,000	4,000	250,000	Undetectable
6	500,000	5,000	300,000	<3,000
7	25,000	5,000	80,000	Undetectable
8	25,000	3,500	120,000	Undetectable
9	25,000	5,000	80,000	<3,000
10	400,000	5,000	100,000	Undetectable
11	250,000	4,000	80,000	<3,000
12	500,000	4,000	80,000	<3,000
13		3,500		
14		8,000		
15		4,000		